LONGER-TERM FEASIBILITY STUDY OF *IN-SITU* IRON AND MANGANESE REMOVAL BY OZONATION: A NOVEL APPROACH TO PROTECTING GROUNDWATER SUPPLY SCHEMES

Final report to

THE WATER RESEARCH COMMISION

by

G. Tredoux, M. Mills, M. Rehman, A. Steyn, P. Ravenscroft, N. Jovanovic

WRC report no. 2528/1/25

ISBN 978-0-6392-0703-2

May 2025

Obtainable from
Water Research Commission
Private Bag X03
Gezina, 0031
Republic of South Africa

EXECUTIVE SUMMARY

BACKGROUND

Borehole clogging due to iron and manganese biofouling is a problem in primary and secondary aquifers in South Africa. As a result, the Water Research Commission (WRC) appointed the Council for Geoscience (CGS) to conduct a study towards resolving this issue, titled "Longer-term feasibility study of in-situ iron (Fe) and manganese (Mn) removal by ozonation: a novel approach to protecting groundwater supply schemes." This project is a continuation and piloting of previous work conducted at the same location by the CGS (Robey, Tredoux, & Chevallier, 2014) (**WRC Report No. 2070/1/14**), a means of preventing clogging of production boreholes at the Atlantis aquifer wellfields in Western Cape Province using an in-situ approach. Most technologies (within the South African landscape) depend on costly surface infrastructure to remove iron and manganese. The study yielded promising results in terms of the applicability of the technology in South Africa.

The main objective of the current study is to demonstrate conclusively on a pilot production scale that iron (Fe) and manganese (Mn) related clogging problems experienced in South Africa can be prevented in a permanent and cost-effective way by means of in-situ ozonation. This treatment is envisioned to reduce the levels of iron (Fe) and manganese (Mn) from the aquifer system (to within aesthetic limits and nuisance levels), with sanitisation of the groundwater in the area (getting rid of pathogens) as an added by-product.

APPROACH

This project involved the innovative use of ozone as an oxidant, which is novel as an in-situ iron removal methodology (South African Patent No. 2015/08887). Inception-engineering designs were compiled, and the treatment plant assembled accordingly. The treatment procedure comprised of injection of ozonated (aerated) groundwater into three (3) boreholes, located at various distances ranging from 4m to 10m up-gradient of the production borehole, in order to allow for Fe and Mn removal (precipitation) in the aquifer.

Field-testing setup allowed for hourly recording of several key parameters such as the water level, temperature and electrical conductivity at several monitoring boreholes, as well as the injection rates in the three injection boreholes, and the dissolved oxygen concentration at two points (within the aeration tank and at injection borehole BH11DNE). Using telemetry, monitoring data was accessible in real time via the internet. The system was installed in the 3 injection boreholes, 2 monitoring boreholes and the aeration tank. This set-up indicated that remote monitoring through system automation and the use of telemetry is effective in reducing manpower and travel costs.

Impact Statement

Over most of the field test period the total iron concentration at the up-gradient monitoring boreholes and the production borehole were approximately 0.2 mg/L. While down gradient of the production borehole the total Fe concentrations varied between 0.3 and 0.4 mg/L. The maximum allowed iron concentration in potable water as per SANS 241: 2015 and World Health Organisation (WHO) guidelines is 0.3 mg/L. According to the results obtained during this project it is clear that injecting ozonated water at up-gradient boreholes was effective in reducing iron concentrations in the aquifer and in abstracted water from the production borehole.

The manganese field tests yielded erratic results (in most cases total and dissolved Mn concentrations were the same for a particular monitoring point), however, laboratory analyses of samples taken at the beginning of November 2019, after ozonation started, consistently gave concentrations of approximately 0.1 mg/L for both total and dissolved manganese. Down gradient of the production borehole total Mn registered 0.2 mg/L; this is the maximum allowed concentration as set out by SANS 241: 2015 and WHO standards.

The results obtained from the field tests confirm the feasibility of in-situ iron removal at 10m from the production borehole. Although the final aim of system parameters for full-scale application was not reached the way ahead is clear and achievable in a follow-up project; the excessive presence of the drilling mud in the subsurface is presumed to attribute to borehole clogging experienced on site. Through continuous pumping of the production and injection borehole it is hoped that the issue will be alleviated (as observed in a monitoring borehole nearby when purged for several hours). Ozone and oxygen injection rates need to be carefully measured and controlled in order to avoid groundwater oversaturation issues such as bubbling. Also, in order to achieve meaningful readings, telemetric and manual measurements should be comparable. There was not enough time to evaluate this discrepancy during this project.

ACKNOWLEDGEMENTS

The project team would like to thank the WRC for making the funds available to carry out this research. The authors would also like to extend their gratitude to the CGS for providing additional funding for the drilling of the injection boreholes, for supplying essential material and for undertaking the soil analyses. In addition, contributions from previous work undertaken by the late Mr Obed Novhe are warmly acknowledged. We also wish to thank Dr Sumaya Israel who provided us with unfailing assistance, even after she had left the project team.

This study would not have been possible without the co-operation and support of the City of Cape Town's Bulk Water Management and the staff at Atlantis Water Works (Softening Plant). We wish to acknowledge, especially, Mr John Charles, Mr Ricardo Swartbooi and Mr Cecil Donnelly. Thank you for allowing us to continue to use production borehole G30966 for longer than we had initially agreed to, and for watching over our site.

The project team would like to offer our thanks to the following members of the Reference Group for their time, advice and willingness to assist: Dr Shafick Adams (Chairman, WRC), Ms Nicolette Vermaak (of the former Department of Water and Sanitation), Prof Esta van Heerden (formerly of the University of the Free State), Ms Jodie Miller (University of Stellenbosch), Mr Terry Harck (Solution H Plus), and Ms Candice Lasher-Scheepers (City of Cape Town).

TABLE OF CONTENTS

LIST OF FIGURES

LIST OF TABLES

LIST OF ABBREVIATIONS/ACRONYMS

CGS	Council for Geoscience
DO	Dissolved oxygen
DWS	Department of Water and Sanitation
EC	Electrical conductivity
ISIR	*In-situ* iron removal
MRWA	Minnesota Rural Water Association
SANS	South African National Standards
TDS	Total dissolved solids
TOC	Total organic carbon
WHO	World Health Organisation
WRC	Water Research Commission

BACKGROUND

Groundwater is one of the most commonly used sources of drinking water worldwide, owing to the natural filtration properties of aquifers. Moreover, groundwater requires much less treatment before use than surface water (Klingel, 2016). As surface water sources in South Africa continue to be placed under increasing pressure, the need to develop groundwater supply schemes is intensifying (Department of Water (DWS), 2010). However, the sustainability of many of these schemes is threatened by the presence of bivalent iron (Fe^{2+}) and manganese (Mn^{2+}) ions in the groundwater (Robey *et al*., 2014). Their occurrence presents challenges related both to water supply (quantity) and quality, with the clogging (and ultimate failure) of production boreholes being the main concern.

Borehole clogging in anoxic aquifers is caused by biogeochemical processes at the borehole screen owing to the ingress of oxygen through pumping. Two examples of borehole clogging in South African wellfields are at the primary Atlantis aquifer in the west coast, and at the fractured Table Mountain Group aquifer at Dysselsdorp. Both schemes were developed to supply domestic rural communities in semi-arid areas with no access to proximal surface water resources. In 2003, the production boreholes of both schemes were operating at less than 30% of their original allocated yields due to iron-related clogging (Flower and Bishop, 2003).

Historically, attempts to recover losses in borehole yields have been found to be costly and only partially successful, and have not provided a permanent solution. The focus has been on resolving the clogging problems and not on treating the direct cause of the problems i.e. the presence of Fe^{2+} and Mn^{2+} ions in the groundwater. Eventually, clogged production boreholes have needed to be replaced at significant cost. The purpose of the present project is to demonstrate conclusively on full production scale that iron-related clogging problems experienced in South Africa can be overcome permanently and cost effectively by eliminating the underlying source. It is envisaged that this will be achieved by removing Fe^{2+} and Mn^{2+} from the groundwater before reaching the production borehole (through a screen and pump mechanism) by changing the redox environment so as to make it unfavourable for Fe and Mn solubility.

In-situ/subsurface bioremediation oxidation techniques have been successfully applied overseas for decades to remove Fe^{2+} and Mn^{2+} in groundwater (Hallberg and Martinell, 1976; Braester and Martinell, 1988; Appelo *et al*., 1999; Van Halem *et al*., 2010). However, these techniques are limited and not well understood in South Africa, hence the need to explore their applicability. Initial field studies carried out in the primary Atlantis aquifer yielded promising results (Robey *et al*., 2014), and the objective of the present project was therefore to carry out full-scale tests in view of developing the necessary engineering design criteria.

In *ex situ* rehabilitation systems, improved borehole performance is maintained for weeks to months. Enhanced *in-situ* bioremediation is considered applicable when the groundwater temperature is between 12 °C and 25 °C and within a pH range of 5–9 (where bacterial growth is observed). Other factors measured include location and season, which are known to accelerate microbial growth. In anaerobic conditions, biofouling controls such as sulphate-reducing bacteria can generate hydrogen sulphide, which, in turn, reacts with Fe and Mn to form metallic sulphides (Plummer *et al.*, 2005).

Treatment is initiated when Fe and Mn concentrations in the production borehole are observed to rise. During injection/treatment, an oxidised zone, free of precipitated solids, is created around the production borehole. *In-situ* iron removal (ISIR) using the Vyredox method entails increasing the oxygen content of the groundwater (Tredoux *et al*., 2004).

When aerated or oxygenated water approaches a borehole, the redox chemistry changes (from reducing subsurface conditions to oxidising conditions), leading to a change in dissolved Fe^{2+} and Mn^{2+} into less soluble Fe^{3+} and Mn^{4+} ions, respectively. Aeration requires the careful control of the water flow; if water flow is excessive and too rapid, not enough air (and/or ozone) is available to oxidise the Fe and Mn. However, if water flow is slow and negligible, the water can become saturated with dissolved oxygen and becomes corrosive to the treatment system (Minnesota Rural Water Association (MRWA), 2019).

Fe and Mn, when oxidised, precipitate as (hydro) oxide according to the equations below (Appelo *et al*., 1999; Portjanskaja, 2010):

$$2Fe^{2+} + O_3 + 5H_2O \rightarrow 2Fe(OH)_3 + O_2 + 4H^+ \quad (1)$$

$$Mn_2+ + O_3 + H_2O \rightarrow MnO_2 + O_2 + 2H^+ \quad (2)$$

Soluble iron Fe^{2+} (called ferrous iron) is oxidised to ferric iron (Fe^{3+}) by ozone. The ferric iron then hydrolyses to form $Fe(OH)_3$, which is a particulate and can be removed by standard filtration or which attaches to surfaces within the aquifer. The oxidation of ferrous iron with ozone takes place at a pH above 7.0, preferably over 7.5. According to equation (1), the reaction of Fe^{2+} to Fe^{3+} consumes 0.43 mg of ozone per 1 mg iron. Iron can also be oxidised by oxygen, but the reaction is much slower compared to ozone owing to the short half-life of ozone. Likewise, soluble manganese (Mn^{2+}) is oxidised by ozone to form manganese dioxide MnO_2, as per equation (2). This process consumes 0.88 mg of ozone per mg of Mn^{2+}, and the optimum pH range for the oxidation of Mn^{2+} to the insoluble form is above 8.0 (wcponline.com).

Ozone is the triatomic form of oxygen. Although oxygen is not detectable by smell, ozone has an extremely low odour threshold. The solubility of ozone is 13 times greater than oxygen, and it is one of the most powerful oxidants on earth. This oxidation potential allows ozone to break down contaminants and kill bacteria more rapidly than most chemical alternatives (oxidationtech.com).

Ozone is more soluble than oxygen, and has been used in municipal water treatment applications for disinfection purposes. It has been identified as a good alternative *in-situ* chemical oxidation compound for soil and groundwater remediation. Ozone sparging (injection into groundwater through a microporous oxidation point) below the water table is a form of an *in-situ* ozone remediation application. The half-life of ozone in the presence of water is typically 30 minutes; however, it can be longer in subsurface environments. Ozonation in these environments is sustained over a longer period owing to the limited mass transfer of the ozone to the groundwater (Plummer *et al*., 2005).

1 INTRODUCTION

Borehole clogging due to Fe and Mn biofouling is a significant problem in primary and secondary aquifers in South Africa. As a result, the WRC has appointed the CGS to conduct a study in view of resolving this issue. The study, culminating in the present report, is a continuation of previous work undertaken by the CGS (Robey *et al*., 2014), the purpose of which is to investigate a means to prevent the clogging of production boreholes at the Atlantis aquifer wellfield in the Western Cape Province.

The main objective of the current study is to demonstrate conclusively, on full production scale, that iron- (Fe) and manganese- (Mn) related clogging problems experienced in South Africa can be prevented permanently and cost effectively by applying *in-situ* ozonation. To date, inception-engineering designs for full-scale testing have been compiled, and the treatment plant has been assembled. Injection runs were implemented after finalising the commissioning of the automated system. The mechanisation of the system (with the treatment operating continuously (24/7) with minimum human labour participation) has facilitated testing and the delineation of the treatment parameters.

This report outlines the work done thus far in order to determine the system parameters for the ozonation treatment of a primary aquifer, including hydrogeological characterisation through drilling and pump tests, groundwater flow and monitoring, water quality and geochemical aspects. The treatment procedure entails the injection of ozonated (aerated) groundwater into three (3) boreholes. First, groundwater is injected into one borehole at a time and then into all three simultaneously (up-gradient of the production borehole) to allow for the removal (precipitation) of Fe and Mn. This treatment is envisioned to reduce the levels of iron (Fe) and manganese (Mn) from the aquifer system (to within desirable aesthetic limits and acceptable nuisance levels), with the sanitisation of the groundwater through the removal of pathogens as an added by-product.

The study area is in Atlantis, a small industrial town located 50 km north of the Cape Town metropole, along the west coast of South Africa in the Western Cape Province (Figure 1). The pilot site is located at the eastern extremity of the farm Kleine Springfontyn, southwest of the town of Atlantis, at the junction of west coast (R27) road and Dassenberg Road (R307). The pilot site was established around a production borehole used by the adjacent softening plant.

The area is characterised by a Mediterranean-type climate and receives polar frontal and cyclonic winter rainfall (Roberts *et al*., 2008). The mean annual rainfall in the area is between 369 and 416 mm, and has been observed to vary monthly and annually (Muller and Botha, 1987).

According to Muller and Botha (1987), the topography near Atlantis and Mamre ranges between 160 and 200 m above sea level. However, the elevation of the pilot site is much lower, at around 55 m above sea level.

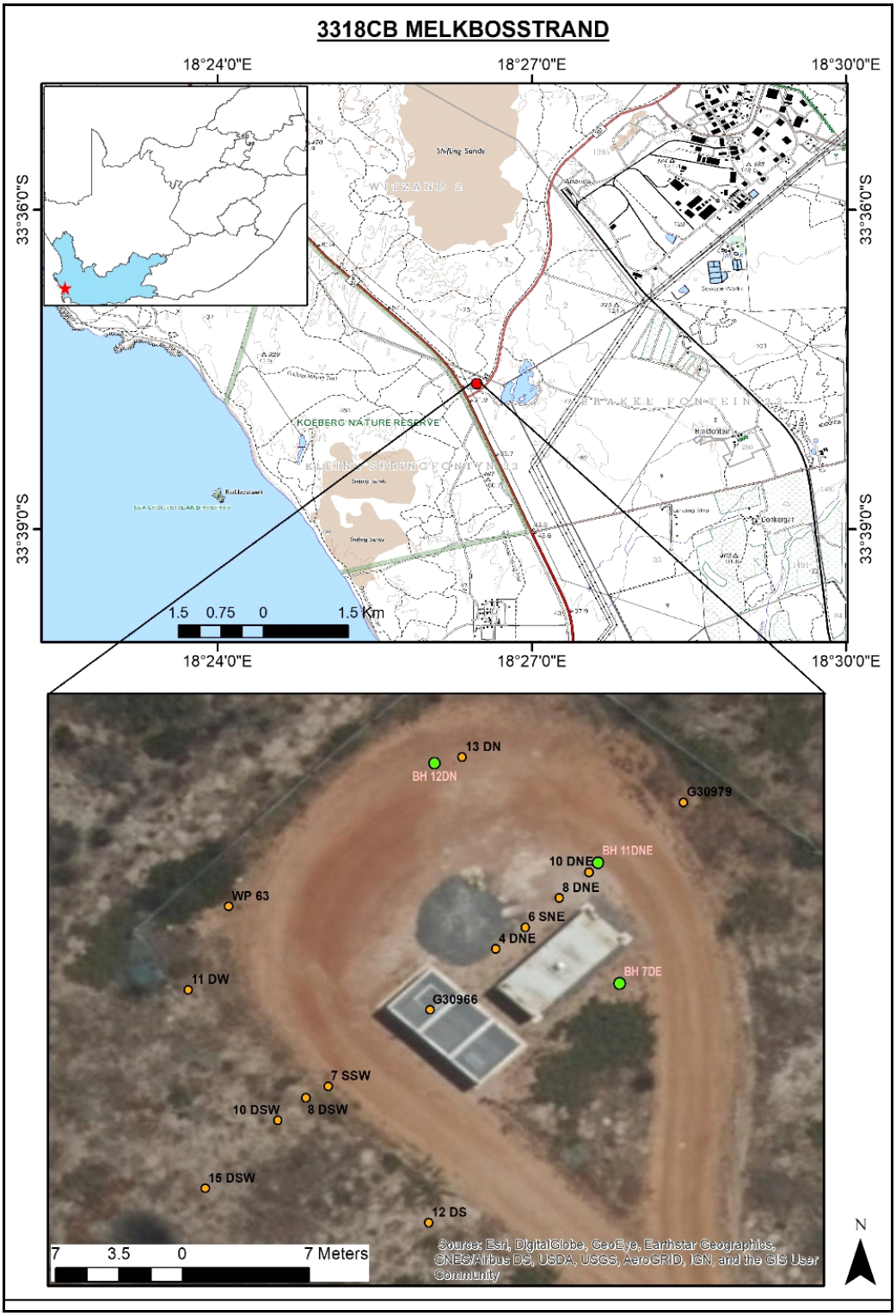

Figure 1. The geographical location of the study area and the aerial view of the pilot site..

2 GEOLOGY

The study area is underlain by the Sandveld Group sediments of Cenozoic age, which, in turn, overlie the basement Malmesbury Shales (Bugan *et al*., 2012). The Sandveld Group consists of unconsolidated to partially consolidated sands constituting the water-bearing strata of the Atlantis aquifer. The Malmesbury Group rocks are the oldest in the area, and form the basal boundary of the Atlantis aquifer (Muller and Botha, 1987).

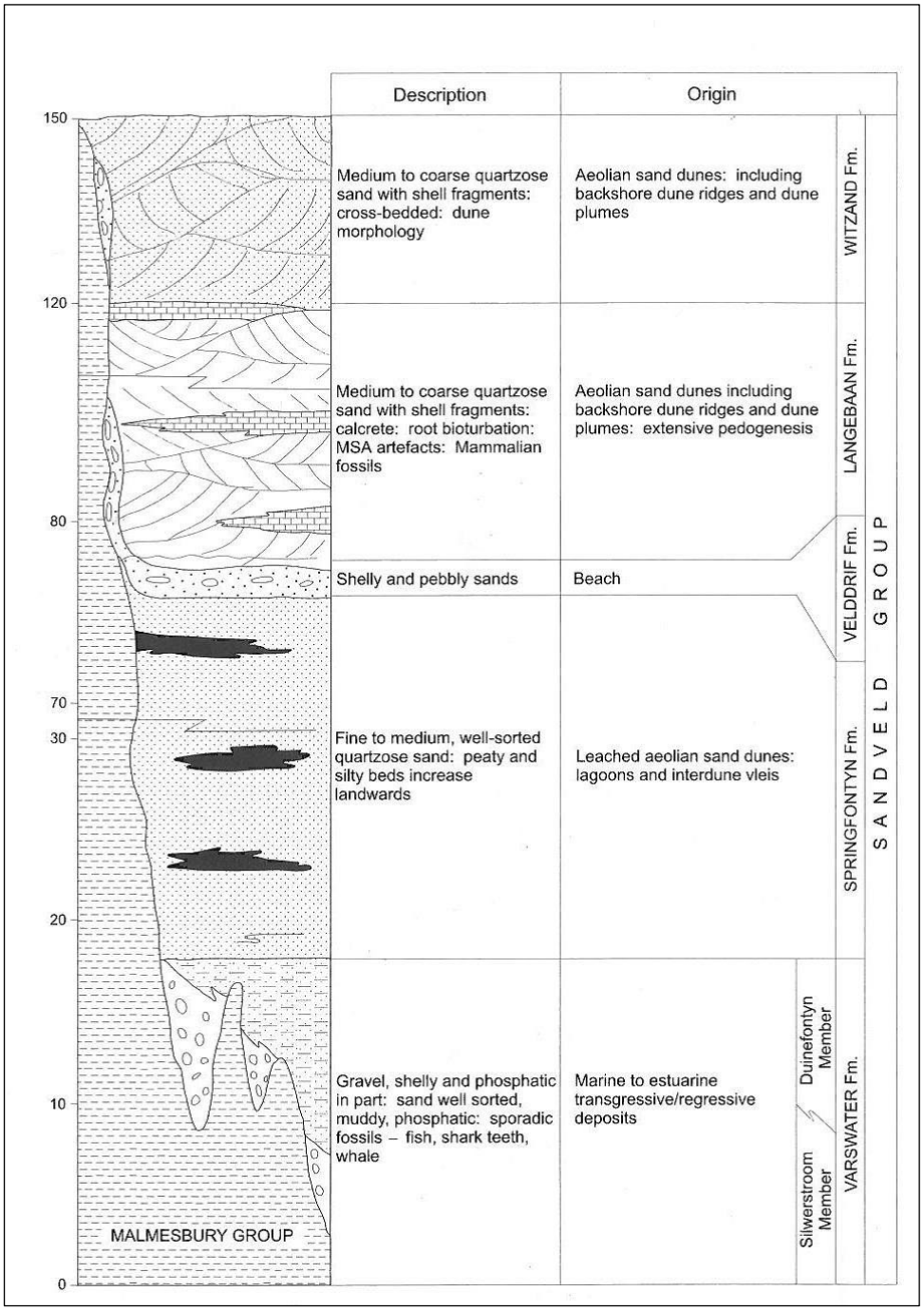

Figure 2. Stratigraphic column of the Sandveld Group (from Roberts, 2001).

According to Roberts (2001), stratigraphically the Sandveld Group is subdivided into the Varswater, Springfontyn, Velddrif, Langebaan and Witzand Formations (Figure 2). These sediments have been deposited since the Cenozoic Era (~90 Ma to present). The strata are thin or absent in the high-lying areas, and the thickest packages are located in basement depressions. Cenozoic strata in the study area can reach a thickness of 50 m, while the basement rocks can attain elevations of 190 m in the vicinity of Mamre in the north (Roberts, 2001).

The 1:50 000-scale geological map of Melkbosstrand (after Roberts, 2001) indicated that the pilot site is located on the Witzand Formation (Figure 3). According to Roberts (2001), this formation consists of unconsolidated calcareous well-sorted, fine- to medium-grained aeolian sands. This uppermost unit of the Sandveld Group rests unconformably on the basement Malmesbury Group in places while, elsewhere, it unconformably overlies the Springfontyn Formation.

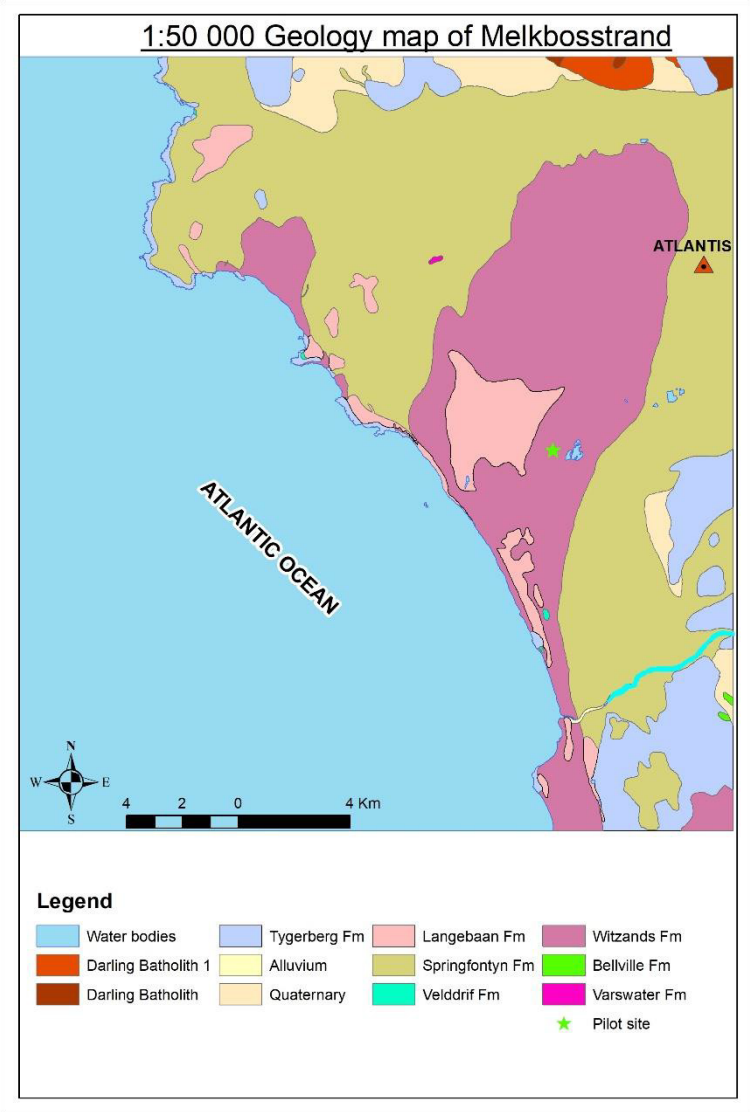

Figure 3. 1:50 000-scale geological map of the study area and surroundings (after Roberts, 2001).

According to Browning and Roberts (2016), the thickness of the Witzand Formation is variable, but is usually less than 30 m. The pilot site is located on the Duynefontein mobile plume that forms part of a group of sporadically distributed coastal dunes along the southern west coast. Cole and Viljoen (2001) described the Springfontyn Formation as comprising well-sorted, fine- to medium-grained unconsolidated quartzose sand.

Borehole G30979 and all the boreholes at the pilot site intercept the basement Malmesbury rocks at around 30 m depth. Betram *et al*. (1984) indicated that the bedrock below G30966 and G30979 is located a height of 20 m above sea level. Lithological profiling of the pilot site exists in the form of drill logs for borehole G30979 (Figure 4). Although the various lithological formations have not been defined, the various sand units have been described.

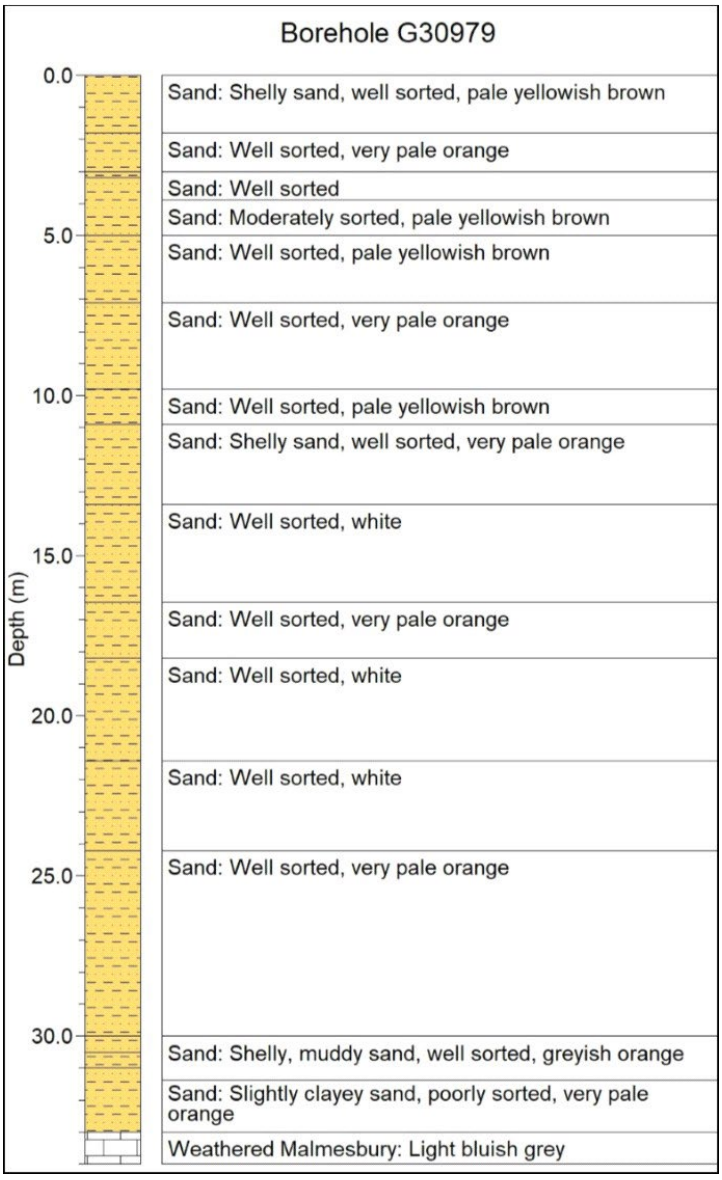

Figure 4. Geological log of monitoring borehole G30979 (Nealer, 1979).

Figure 5 depicts the spatial distribution of all the boreholes at the pilot site; production borehole (G30966) around which the project is centred, monitoring boreholes (G30979, and WP63), injection and monitoring boreholes from the previous project (BH4DNE, BH6SNE, BH8DNE, BH10DNE, BH13DN, BH7SSW, BH8DSW, BH10DSW, BH15DSW, BH12DS, BH11DW), and newly drilled boreholes (BH11DNE, BH12DN, BH7DE).

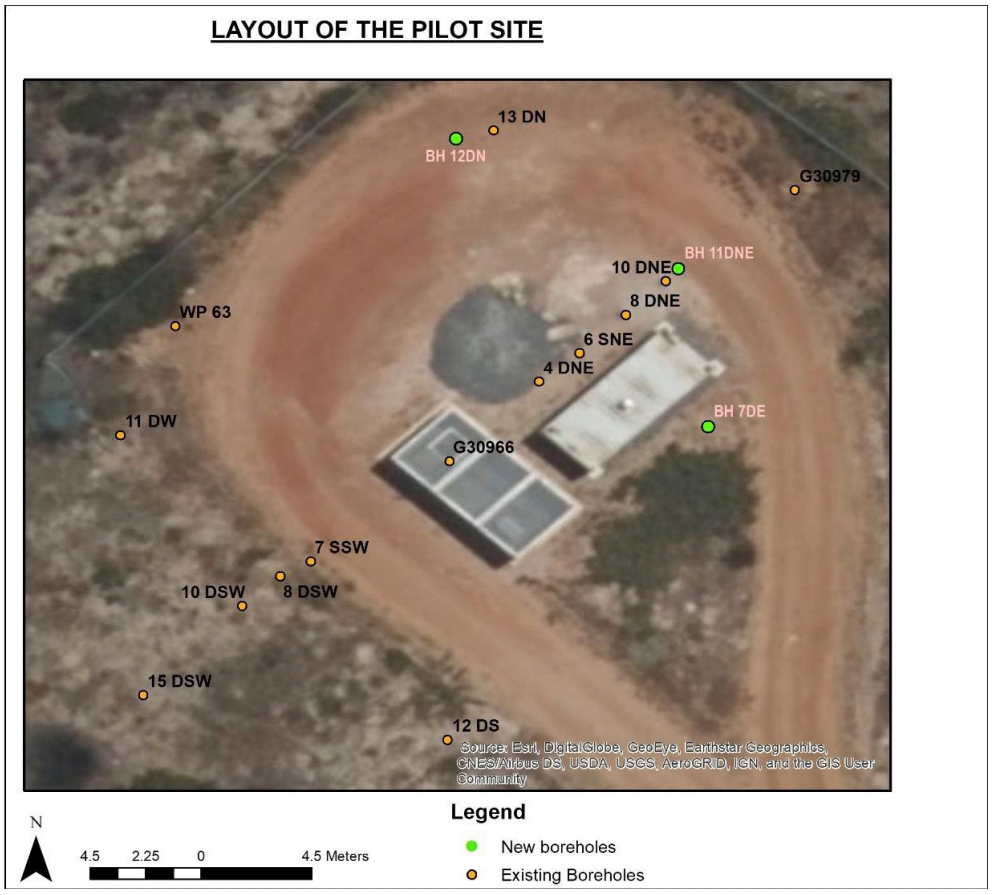

Figure 5. Spatial distribution of the boreholes at the pilot site.

An investigation of the engineering designs revealed that the sizes of the existing boreholes were not sufficient to accommodate the requisite injection pipework. Thus, new boreholes were drilled. Although during the present and the previous projects, several boreholes were drilled, these could not be properly logged as mud-rotary drilling adversely affects this process (Figure 6). From 28 May to 8 June 2019, SA Rotsbore Drilling Company drilled three new boreholes with larger diameters (2 x 113 mm and 1 x 143 mm).

Figure 6. Muddy, indistinguishable drill samples from mud-rotary drilling at the pilot site.

As the new boreholes were intended to replace the existing boreholes, they were drilled one metre away from the previous boreholes (for BH11DNE, and BH12DN) while borehole BH7DE was positioned away from the gravel road on-site, and closer to the production borehole. The new boreholes were positioned 11, 12 and 7 m away from the production borehole.

Most of the boreholes (with the exception of BH6SNE and BH7SSW, which are 15 m deep) were drilled to a depth of 33 m, and cased and capped at 31 m. The perforated screen in each borehole was fitted from 24–31 m to mirror the production borehole (G30966). The three recently drilled boreholes were gravel packed. Airlifting was applied at the boreholes in order to expel the mud that had been introduced during drilling.

3 HYDROGEOLOGY

The water-bearing strata of the Cenozoic deposits in the 1:50 000-scale Melkbosstrand mapped area constitute what is widely known as the Atlantis aquifer (also referred to as the Silwerstroom–Witzand unit by Meyer, 2001). All the production boreholes of the Witzand wellfield are located within this aquifer, targeting the Springfontyn Formation (Van Der Merwe, 1980). The wellfield is bounded from below by the basement rocks and by the coastline on the west and pinches out in the north, east and south (Muller and Botha, 1987).

The Atlantis aquifer is a coastal intergranular aquifer, as opposed to the alluvial intergranular aquifers in the greater 1:500 000-scale Cape Town area. Specific to this aquifer is its low storage capacity of 400 (mm^3), a good comparable recharge of about 15–35% of mean annual precipitation, high transmissivity values that reach 1 300 m^2/day, and a general sodium-chloride-calcium-alkaline nature (Meyer, 2001).

Coastal aquifers are generally unconfined, prone to contamination, and drain towards the sea. Overabstraction and mismanagement of this type of groundwater resource usually result in seawater intrusion. Betram *et al.* (1984) indicated that groundwater levels in the Atlantis aquifer follow the topography and the groundwater drains into the Atlantic Ocean in the west.

According to Tredoux and Cavè (2002), the Atlantis aquifer appears to be semi-unconfined in places due to varying hydraulic conductivities (K). There is evidence of delayed yields as a result of the presence of calcrete lenses. An average K-value of 2.1 m/day for the entire Witzand wellfield is postulated. Fleisher (1990) described the aquifer as being phreatic, heterogeneous and anisotropic.

Figure 7 depicts the 1:50 000-scale hydrogeological map of the Melkbosstrand area. The map delineates the different aquifer types, the surface water resources and various existing groundwater features such as springs and rivers.

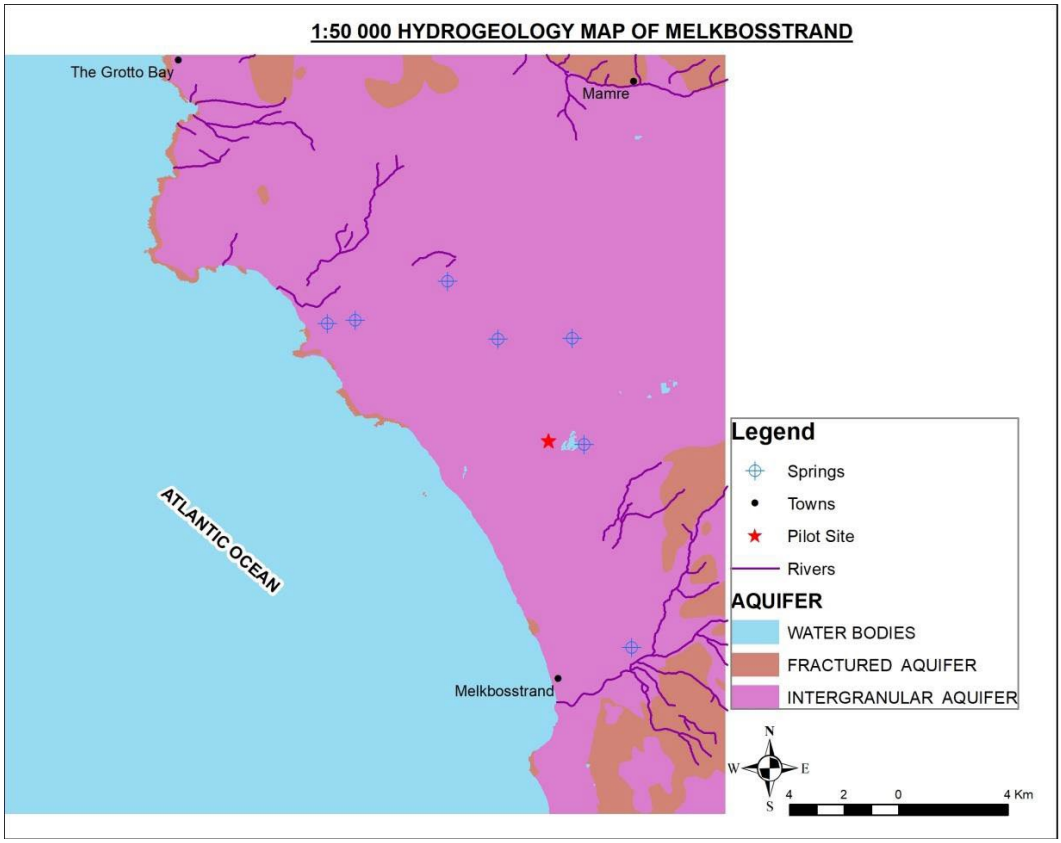

Figure 7. Regional hydrogeological map of the 1:50 000 Melkbosstrand map area (after Meyer, 2001).

Robey (2014) summarised the parameters of the historical aquifer for the study area, ranging from when the production borehole was first drilled. Table 1 presents these data as well as the updated information from the last constant discharge test performed on the production borehole (Robey, 2014). The data seem to depict an increase in hydraulic properties of the aquifer from when it was first drilled, as manifested in the transmissivity and storativity, while yield has decreased from 9.72 to 5 L/s at present (51% performance/pumping reduction).

Table 1. Historical and recent hydraulic properties of borehole G30966.

T(m^2/d)	Storativity	Yield (L/s)	Reference	Year
556	0.004	9.72	Van Der Merwe	1980
280	0.14		Bredenkamp *et al.*	1982
		5.50	Cavè	1997
		5.00	More Water	2001
		7.00	Bugan *et al.*	2012
600	0.20		Robey	2014

Traditionally, transmissivity and storativity values are calculated from a constant discharge test using the Theis and or Theis–Jacob non-steady state methods. Without using the pump test results, hydraulic conductivity can be calculated, using the equation:

$v = -Ki$ (3)

where v is specific discharge, K is hydraulic conductivity and i is hydraulic gradient. However, specific discharge will need to be known, and was not determined during this exercise.

In an unconfined aquifer, the storativity relates to specific yield, and ranges from 0.1 to 0.3 (Lohman, 1972). According to Bear (1979) specific yield is less than total porosity in an unconfined aquifer, while Heath (1983) gives the porosity of sand a value of 25 (percentage volume) and specific yield value of 22 (percentage volume). The computed storativity value of the Atlantis aquifer (at the pilot site with a thickness of 35 m) is 4.1×10^{-3} (using the equation: $S = Ssb = pg(\alpha + n\beta)b$, where S is storativity, Ss is specific storage, b is aquifer thickness, p is density of water, g is gravity, α is aquifer compressibility, n is total porosity, and β is water compressibility).

4 PUMP TEST AND ANALYSIS

A pump test may be performed to determine the hydraulic characteristics of the water-bearing layer(s) of an aquifer, or to provide information about the borehole yield and drawdown (Kruseman and Ridder, 2000). This project seeks to understand the productive capacity of the production borehole by determining the hydraulic characteristics of the Atlantis aquifer. A step-drawdown test was carried out prior to starting ozone injection to quantify the aquifer baseline hydraulic characteristics, and the results are presented below.

The five (5) hour step-drawdown test was conducted on the production borehole on 8 August 2019. Each step took 60 minutes to complete, and the recovery took approximately 130 minutes. Two monitoring boreholes were used during the test, one up-gradient of the production borehole (BH10DNE) and the other down-gradient (BH10 DSW), at a distance of 10m from the pumped borehole.

The technical staff of the Atlantis Water Scheme of the City of Cape Town performed the step- drawdown test using a variable speed gauge and the submersible pump that had already been fitted in the production borehole. A 100 m long lay flat (pipe) was attached to the borehole in order to drain water away from the borehole into a nearby down-gradient vlei. A flow meter attached to the production borehole was used to measure flow rate, while water level readings were taken using dip meters (manual readers).

The variable gauge was used to increase the speed and, thus, the flow rate, every 60 minutes, over the 60 minute duration. Owing to a lack of staff (the test was performed during a shutdown in the province which affected staff availability), the first hour of testing was not monitored as would normally have been the case, with increasing intervals between readings. The readings were conducted at 10 minute intervals, adapted to local conditions. The discharge point of the lay flat was located too far from the monitoring borehole for the available staff to conduct discharge rate measurements.

G30966 had previously been pump tested in January 2013 using the step-drawdown method, and in April 2013 using the constant discharge method. The results of the latest (2019) step-drawdown method were not as expected (there was an increase in specific capacity with time), bringing into question the accuracy of the data and the methodology for gathering and recording the data.

Table 2 shows the results of the step-drawdown test performed on G30966 in August 2019. The subsequent graphs are displayed in Figure 8. The overall shape of the curves for the production borehole and for the monitoring boreholes is typical for a step- drawdown test (Van Tonder *et al*., 2001), albeit with a few anomalies noted especially in monitoring borehole 10DNE. There is an observed increase in drawdown with an increase in time (in each step, and overall), and all the boreholes appear to recover to within the range of static water levels.

Table 2. Step-drawdown data for borehole G30966 for August 2019.

Step 1			
Interval (min)	Water level observations (m):		
	G30966 (Production	10 DNE (Observation	10 DSW (Observation)
0	5.30	4.75	5.60
10	10.39	5.20	5.51
20	10.40	5.22	5.51
30	10.43	5.23	5.51
40	10.43	5.24	5.52
50	10.44	5.23	5.52
60	10.43	5.25	5.52
Step 2			
	G30966 (Production	10 DNE (Observation	10 DSW (Observation)
70	11.24	5.25	5.60
80	11.28	5.29	5.60
90	11.28	5.31	5.61
100	11.28	5.32	5.61
110	11.29	5.32	5.61
120	11.29	5.33	5.62
Step 3			
	G30966 (Production	10 DNE (Observation	10 DSW (Observation)
130	12.04	5.25	5.62
140	12.06	5.37	5.69
150	12.06	5.38	5.69
160	12.07	5.39	5.69
170	12.07	5.40	5.69
180	12.05	5.40	5.69
Step 4			
	G30966 (Production	10 DNE (Observation	10 DSW (Observation)
190	12.60	5.40	5.70
200	12.60	5.42	5.75
210	12.60	5.42	5.74
220	12.57	5.43	5.75
230	12.57	5.44	5.75
240	12.57	5.44	5.75
Recovery			
	G30966 (Production	10 DNE (Observation	10 DSW (Observation)
250	12.57	5.44	5.75
260	5.34	4.83	5.11
270	5.34	4.85	5.10
280	5.34	4.80	5.10
290	5.33	4.80	5.09
300	5.33	4.80	5.09
310	5.33	4.80	5.11
320	5.32	4.79	5.09
330	5.33	4.79	5.11
340	5.34	4.79	5.23
350	5.33	4.79	5.10
360	5.32	4.79	5.07
370	5.32	4.79	5.08
380	5.32	4.79	5.08

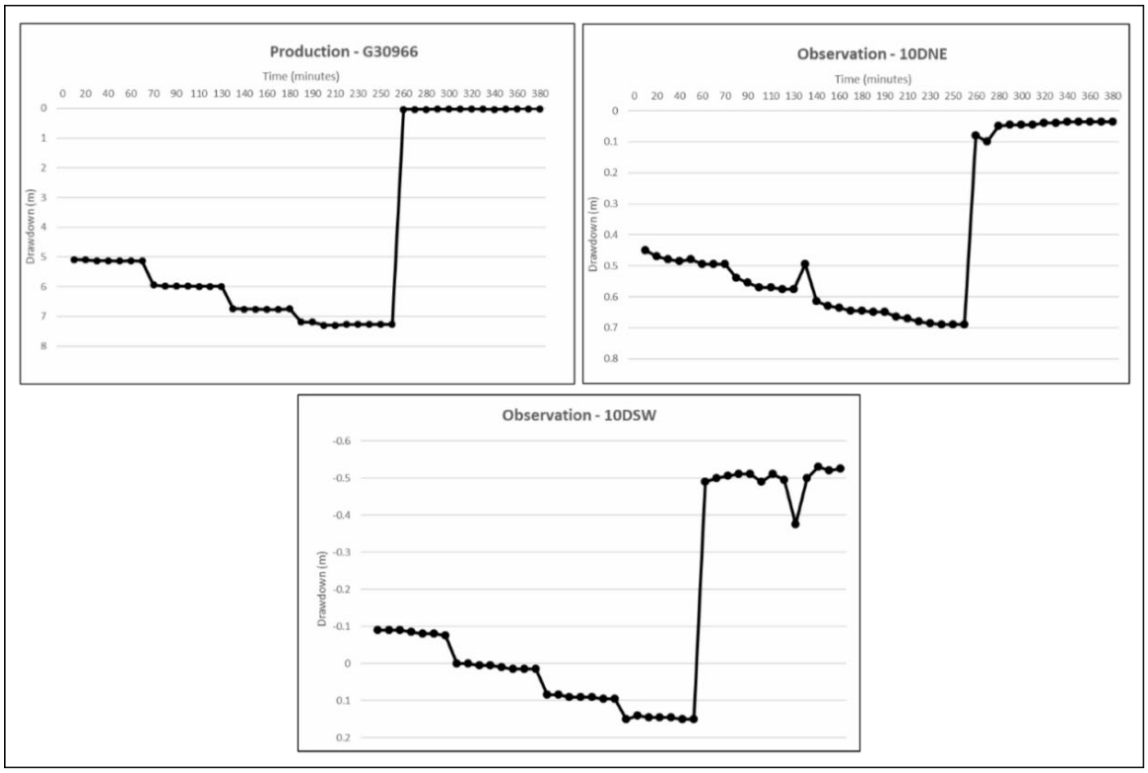

Figure 8. Step-drawdown curves for the production and monitoring boreholes.

Judging by the poor response, as well as the rest water level of 4.75 m and the increase to 5.20 m in the observation borehole 10DNE, it is highly likely that the production borehole was clogged. However, the water levels in 10DNE two days prior to pumping were 4.72 m and 4.78 m for 6 August and 7 August 2019, respectively. There was a massive quantity of drilling mud residue in 10DNE when it was first sampled after the drilling of the nearby 11DNE. This may explain the suspected clogging effects seen during pump testing.

Monitoring borehole 10DSW produced unexpected results — the rest water level appeared to be deeper than for the entire first step of the pump test. This may have been the result of human error, since the rest water level taken a day prior to testing was recorded at 5.08 m and at 5.60 m on the day of the pump test. The second step is seen to start at the rest water level, a behaviour in line with the first step. Overall, the behaviour was congruent with a borehole during a pump test, although the time-drawdown curve plotted above the rest water level.

Production borehole G30966 and monitoring borehole 10 DNE were seen to recover to within the rest water levels, while borehole 10DSW was seen to recover significantly above its rest water level. Although the flow meter installed in the production borehole was used to give flow rates during the test, these were omitted from Table 1 as they were regarded as questionable.

During each step, the pumping rate using the variable gauge was increased, however manual flow rates for these steps were inconsistent (the flow rates were recorded as 9.94, 5.95, 12.8, and 7.07 for the steps respectively). No piezometer had been installed in either the pump or monitoring boreholes during this test. The increased flow was corroborated by the water level readings and resultant time-drawdown curves. Perhaps pressure adjustments had not been considered before taking the flow readings, as was later observed for the types of flow meters used.

During the 2013 step-drawdown test (Robey, 2014), a significant decline was noted in the production borehole during the first minute (referred to as borehole loss). The same was noted during the present project (as is evident from Table 2) where there is a 5m drop from the rest water level. The borehole loss was thought be the result of clogging or screen collapse.

No follow-up investigations such as camera logging or removal of the pump were undertaken to verify the clogging or screen collapse. However, currently the borehole is still operational and pumping at a sustained rate (although at a much lower rate than the initial rate achieved when the borehole was first drilled) seven years later. Based on this and the previous step-drawdown test results, similar responses indicate that borehole performance is unchanged and that there is thus no loss in borehole performance (until before the start of injection).

5 GROUNDWATER FLOW AND MONITORING

Regionally, groundwater flow in the Atlantis aquifer is a response to gravity with the water flowing towards the sea (Meyer, 2001). However, at a local scale, groundwater flow is towards the production borehole, as a result of pumping. Figure 9 shows the 3-D groundwater level flow direction and locations of the different boreholes. There are two distinctive water sinks, one around the production hole attributable to pumping, and another "natural" sink around borehole 11DW where the ground level dips off slightly. The topography at the pilot site is relatively flat, and the associated groundwater response (slight southward dip) is shown in Figure 10.

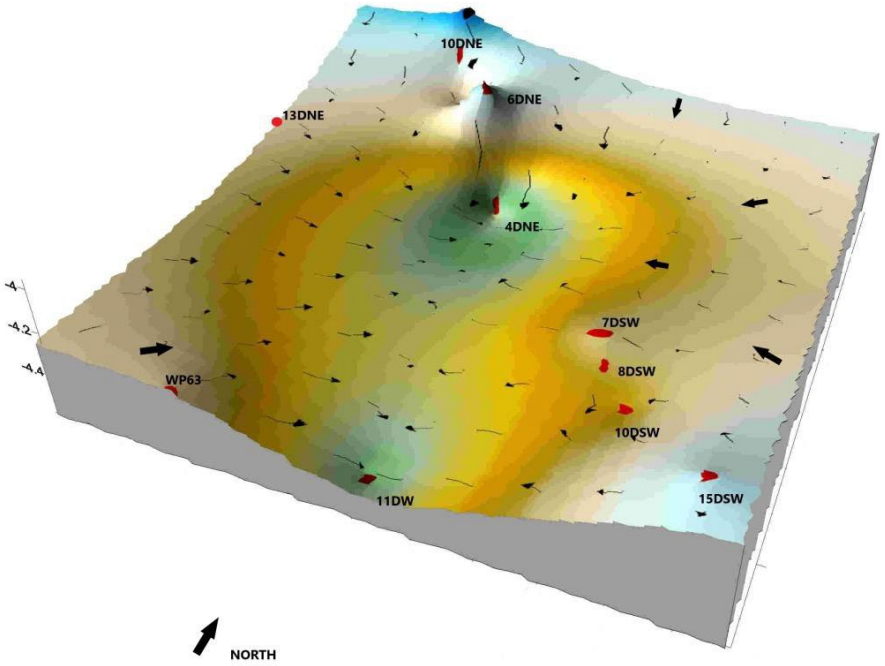

Figure 9. 3-D groundwater representation of pilot site.

The vertical scale has been exaggerated for better visualisation and full effect of the water level decline due to pumping, and to emphasise the visual effects of pumping since the gradient of the water table and the topography is very low (centimetre differences). Figure 9 is based on readings taken during the summer season (24 January 2019).

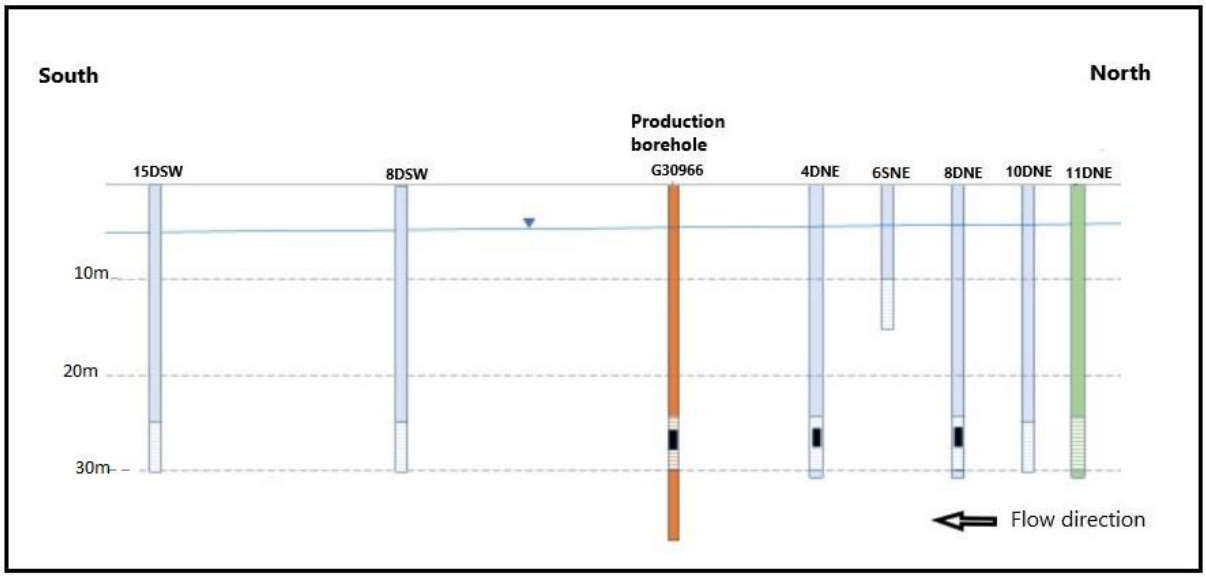

Figure 10. Cross-section of the pilot site boreholes along the production borehole line.

At the inception of the project in 2017, a groundwater monitoring programme for the pilot site was set up. During the pilot phase of the project in 2013, treatment was interrupted by shallow groundwater levels. It became necessary to monitor the groundwater levels in order to attempt to plan ahead in order to circumvent shallow levels.

Groundwater level and basic water quality data were recorded for all the boreholes, including wellpoint WP63. The monitoring was set up at a weekly frequency, and data were collected in the mornings of every Tuesday or Wednesday. However, over time lack of access to the site owing to paperwork delays, drilling and laying of pipework caused interruptions and adversely affected the monitoring programme at various stages.

Table 3 lists the statistical analyses of monitored static water levels around the pilot site indicating shallow levels (with a lowest recorded level of 1.9 m) from borehole G30979 on 2 December 2019). The deepest recorded level was around 11.71 m from the production borehole on 26 February 2020. The maximum recorded reading had, however, been taken while the pump was still switched on.

Table 3. Statistical groundwater level data for the pilot site.

	Number of observations	Min	Date of observation	Max	Date of observation	Average
10DNE	46	2.53	23-Mar-17	5.59	4-Mar-20	4.08
10DWS	45	2.79	3-Feb-17	5.87	4-Mar-20	4.46
11DNE	7	1.26	2-Dec-19	5.69	11-Mar-20	4.06
11DW	44	2.91	23-Mar-17	5.9	8-Aug-19	4.46
12DS	43	2.75	23-Mar-17	5.84	4-Mar-20	4.29
13DN	40	2.56	9-Mar-17	5.47	4-Feb-20	4.03
15DSW	46	2.58	23-Mar-17	5.47	4-Mar-20	4.14
4DNE	44	2.67	23-Mar-17	6.7	11-Jan-19	4.68
6SNE	46	2.64	23-Mar-17	5.32	4-Mar-20	4.07
7DE	8	4.06	11-Mar-20	5.51	21-Jan-20	4.80
7SSW	46	2.7	23-Mar-17	5.52	4-Mar-20	4.28
8DNE	44	2.61	23-Mar-17	5.97	4-Mar-20	4.32
8DSW	46	2.76	3-Feb-17	5.99	4-Mar-20	4.43
G30966	25	2.53	9-Mar-17	11.71	26-Feb-20	7.32
G30979	40	1.9	2-Dec-19	5.66	4-Mar-20	3.91
WP63	39	3.08	14-Jun-17	5.6	8-Aug-18	4.42

The greater Western Cape Province experienced severe drought during the monitoring period. Time series curves of the monitoring data (represented in Figure 11) indicate a lowering of groundwater levels in the study area over this period. According to this graph, the effects of the drought (natural responses attributable to evaporation and evapotranspiration, as well as responses to anthropogenic activities such as increased regional groundwater abstractions from the nearby Witzand wellfield) are represented by declining water levels.

Weather conditions have since recovered, and 2018 and 2019 presented wetter winters in the Western Cape Province. However, groundwater trends, according to Figure 11 still show a decline, with late responses to recharge by the aquifer (as well as increased groundwater use because of the drought). These lower groundwater levels are favourable for the injection of ozonated water to the subsurface. The aquifer is able to receive injected amounts without producing backflow to the ground surface, as had been experienced during the first pilot project.

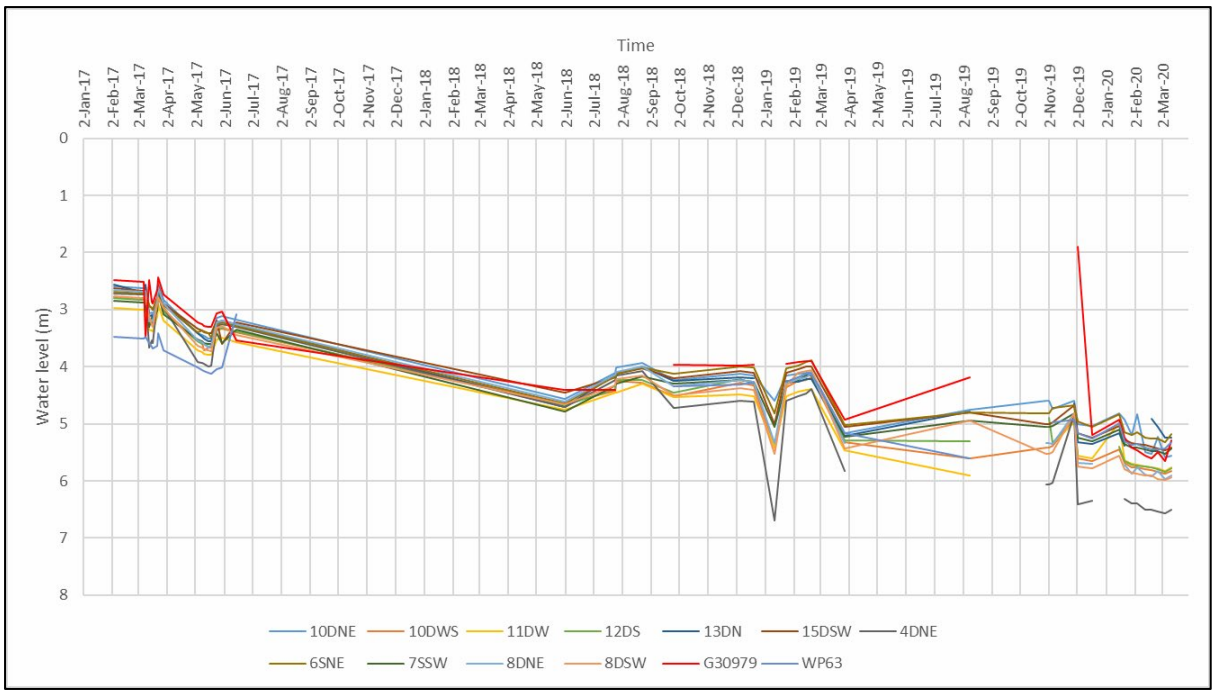

Figure 11. Time series graph for monitored water levels at the pilot site.

6 GROUNDWATER QUALITY ANALYSES

The quality of water in a well is a function of the location of the well screen in the groundwater system and the geochemical conditions around the well screen (Heath, 1983). The water quality for the Atlantis aquifer is influenced by the surroundings, lithology, vegetation and artificial recharge. The various formations of the Sandveld Group have resulted in hard groundwater owing to the calcretes of the Witzand Formation, and iron and sulphates from the peat lenses of the Springfontyn Formation. (Tredoux and Cavè, 2002). Drilling mud residue from recent drilling exercises at the pilot site and the Atlantis aquifer has introduced more organics to the subsurface, thereby affecting the water quality.

It is essential to understand the water content of the aquifer before embarking on any treatment activity such as *in-situ* Fe and Mn removal. High dissolved concentrations of Fe and Mn in the groundwater can cause aesthetic issues and the presence of Fe in an aquifer environment can result in borehole clogging when complemented by the presence of iron bacteria (Tredoux *et al*., 2004).

Mobilisation of Fe and Mn in groundwater occurs under reducing and low pH conditions, and in the absence of sulphide or carbonate ions. The oxidation of iron decreases when it occurs as complexes of silica, phosphate or dissolved organic carbon. The oxidation of manganese, on the other hand, increases with higher pH or microbial activity (Robey, 2014).

Monitoring and maintenance may be applied to mitigate and circumvent borehole clogging in a water supply scheme set-up. The Atlantis Water Resource Management Scheme has been implementing this since experiencing clogging complications Table 4 summarises the different key analytes and the minimum allowed concentrations for drinking water, as indicated by the South African Bureau of Standards (in the latest SANS 241-1:2015) and World Health Organisation (WHO) (2017).

Table 4. Chemical statistics for borehole G30966 for the period 1979–2020 (data supplied by the City of Cape Town).

	Number of observations (n)	Min	Max	Median	SANS 241:2015	WHO (2017)
Physical and aesthetic determinands (mg/L)						
pH	279	6.7	9.5	7.5	≥5 to ≤9.7	-
EC (µS/cm)	286	49.3	144	96	≤170	-
Total Dissolved Solids	240	330.3	902	606	≤1 200	-
Hardness	203	144	788	242	-	-
Chemical determinands — macro-determinands (mg/L)						
Total Alkalinity	256	72	261	179.5	-	-
Potassium	278	0.01	10.7	2.7	-	-
Potassium	278	0.01	10.7	2.7	-	-
Sodium	246	41.5	188	90.5	≤200	≤200*

	Number of observations (n)	Min	Max	Median	SANS 241:2015	WHO (2017)
Calcium	246	40.1	272	76	-	-
Magnesium	246	5	26	10	-	-
Chloride	265	52	285	160	≤300	-
Fluoride	61	0.02	0.6	0.3	≤1.5	≤1.5
Sulphate	239	2	385.8	47.7	≤500 ≤250*	≤250*
Nitrate as N	209	0.001	0.3	0.05	≤11	≤11
Nitrate as N	209	0.001	0.3	0.05	≤11	≤11
Chemical determinands — micro-determinands (µg/L)						
Total Iron	219	27	18 600	519	≤2 000 ≤300*	≤300*
Manganese	110	6	827	196	≤400 ≤100*	≤100*
Aluminium	61	1	196	17	≤300	-
Copper	44	1	45	6.5	≤2 000	≤2 000
Organic determinands (mg/L)						
Total organic carbon (TOC)	33	3.7	7.2	5.1	≤10	-

*Aesthetic guideline value.

This comprehensive monitoring database may aid in the development of treatment blueprints for *in-situ* Fe and Mn removal from groundwater. Almost every month since 1979, water samples from this borehole have been submitted for lab analysis. The pH values (average) are within the range for Fe removal by oxidation, and can be as high as the recommendation for manganese removal. According to Reckhow *et al*., 1991), the oxidation of iron (Fe) requires near-neutral pH (ranges between 7.2 and 8), if manganese is present the minimum pH should be 9.5.

Figure 12 presents a time series curve of the data, with individual values, extending from 1979 to the present. Some years were skipped while, sometimes several samples were analysed for the same month. Total dissolved solids (TDS) started high, and then a hiatus of about 12 years occurred with (unaccounted for) missing values. The trend before the hiatus was declining — especially around 2013 when iron removal treatment was first introduced to the system — but then started to increase again. This saw an introduction of record low values for TDS. The TDS and other values were affected by the artificial recharge regime of the Atlantis aquifer, and the import of low salinity water from the surface water supply system (implemented by the Bulk Water Authority).

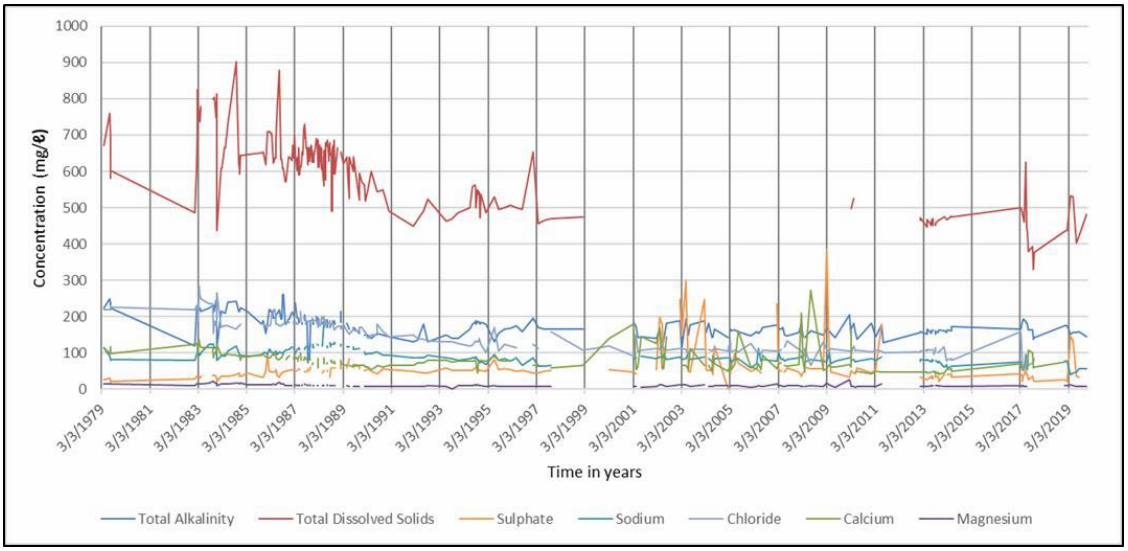

Figure 12. Time series curve of chemical analytes for borehole G30966.

(Total) Fe and (total) Mn were plotted separately as they are the main contaminants in the system (Figure 13). Manganese was not always determined, and was only included in the analysis from 2001 (when clogging problems were first detected). Total Fe is generally low at less than 1 000 µg/L (as noted in the trend of the graph), although there is a large range in values (0–18 000). However, when precipitated iron in the production borehole is dislodged and ends up in the sample, total iron is affected and dissolved iron is used. According to Table 4, the median Fe and Mn values at the production borehole are below SANS limits.

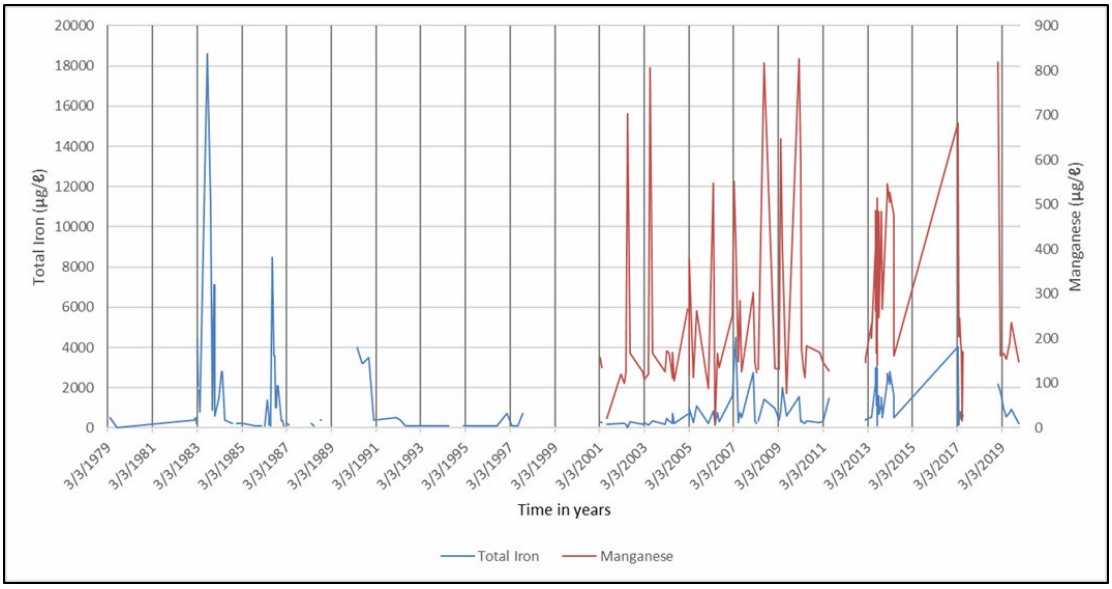

Figure 13. Time series curve of Fe (total) and Mn (total) concentration monitoring.

Field measurements (basics such as pH, EC and temperature), have been collected as part of a background data collection exercise for the pilot site since 2017. These parameters give an

idea of possible clogging conditions and of the suitability of the groundwater for *in-situ* Fe and Mn removal treatment.

Table 5 represents the monitoring data for all the existing boreholes at the pilot site over a two year period. Groundwater samples were extracted from the boreholes and analysed on-site using a multivariable gauge or multimeter, fitted with individual probes for the different parameters. Water was drawn from each borehole using a 12-volt (3 ampere, 2 cm diameter) submersible pump, and several pumps were used during the course of the monitoring as they tended to become clogged over time.

Several sampling methods were explored, in order to improve data accuracy, such as using a bigger submersible pump that could lift water from a deeper depth (25 m) and even using a peristaltic pump. Securing field sampling equipment has been an on-going challenge during this project and, thus, the number of background field measurements is low. However, this number increased when injection started and flow sampling was conducted and field parameters monitored until the measurements stabilised.

Table 5 indicates a significant variation in EC values (minimum ranges from 305–737, and maximum ranges from 469–969). This variance cannot be easily explained as the pilot site is small and is unlikely to host such variety, and the same meter was used throughout sampling.

Since the first injection treatment in October 2019, weekly sampling runs were done and on-site analysis was carried out. The sampled boreholes included G30979 (although this borehole is located outside of the oxidation zone), BH10DNE, BH8DNE, BH6DNE, BH4DNE, production borehole G30966 and BH8DSW. Off-site analysis was carried out at the campus laboratory of the University of the Western Cape, which is not accredited). These results were used as a validation and quality control tool.

Table 5. Field parameter statistics for the pilot site.

Parameter	pH	EC (µS/cm)	DO (mg/ℓ)	Temp (°c)
10DNE				
Number of observations	15	15	14	15
Min	7.23	644	0.02	17.7
Max	7.61	739	20	20.5
Average	7.41	699.49	8.18	19.50
8DNE				
Number of observations	14	14	14	14
Min	7.09	586	0.03	18.6
Max	7.76	719	20	21.2
Average	7.39	686.79	7.15	19.68
6SNE				
Number of observations	14	14	14	14
Min	7.3	657	0.03	19.2
Max	7.82	772	7.83	20.4
Average	7.47	710.43	2.06	19.84
4DNE				
Number of observations	14	14	14	14
Min	7.2	637	0.03	18.7
Max	7.6	697	12.85	19.8
Average	7.35	666.36	2.50	19.41
G30966				
Number of observations	13	13	12	13
Min	7.47	686	1.83	18.3
Max	8.05	724	6.7	19.9
Average	7.58	713.77	3.84	19.18
8DSW				
Number of observations	14	14	14	14
Min	7.43	631	0.01	18.2
Max	7.76	688	0.6	19.1
Average	7.61	666.57	0.19	18.69
G30979				
Number of observations	9	9	4	9
Min	8.3	558	0.08	18.8
Max	8.63	626	0.19	19.2
Average	8.48	596.22	0.11	19.06

Table 6 summarises these results, where the total Fe and Mn were measured on-site and off-site (the two results do not agree), and other essential field parameters were included. The noted discrepancy between the on-site and campus Fe (total) results is attributed to the analyses having been carried out a month apart. According to Israel (2020, personal communication) a fresh sample contains little or no precipitate, hence all iron is in Fe^{2+} form. Israel further explained that if a sample stands for more than a month, a large amount of precipitate forms and there is thus a possibility that the total Fe measurement is slightly higher after a month has lapsed.

At the beginning of treatment and sampling, large quantities of drilling mud residue were noted in the groundwater. The project team resolved to take out the injection equipment from the new boreholes and to purge them until they ran clear. Samples were taken and sent for TOC analysis (at BEMLAB, where total Mn and dissolved Mn were also analysed). The results are also included in Table 6.

Table 6. Statistics of chemical field data for the pilot site.

Date	BH ID	Sampling and analysis result (mg/ℓ)									
		Total Fe	Total Fe*	Dissolved Fe	Total Mn	Dissolved Mn	TOC	pH	EC (µS/cm)	DO	Temp (°c)
7-Aug-19	10DNE	-	-	-	-	-	-	7.54	739	-	17.7
	G30966	-	-	-	-	-	-	8.05	686	-	18.3
1-Oct-19	10DNE	0.01	0.1	0	-	1.4	-	7.23	673	0.02	18.7
	8DNE	0.78	1.41	-	-	0.9	-	7.27	651	0.03	18.6
	6SNE	0.01	0.16	-	-	0.8	-	7.40	693	0.03	19.2
	4DNE	0.54	1.08	-	-	1.5	-	7.30	640	0.03	18.7
29-Oct-19	10DNE	0.13	-	0	-	-	15.4	7.25	704	10.90	19.4
	8DNE	0.02	0.16	0	-	0.8	-	7.10	705	8.33	19.3
	6SNE	0.01	0.03	0.05	-	0.9	-	7.60	772	0.19	19.2
	4DNE	0.03	-	0.09	-	-	15.7	7.60	650	0.17	18.9
1-Nov-19	10DNE	0.13	0.55	0	0.12	0.1	12.5	7.25	704	10.90	19.4
	8DNE	0.02	0.06	0	-	1.6	-	7.09	705	8.33	19.4
	6SNE	0.05	0.04	0.05	-	1.5	-	7.32	679	0.81	19.2
	4DNE	0.01	0.01	bdl	0.07	1.3	3	7.32	697	12.85	19.4
	G30966	0.21	0.39	0.21	-	1.6	-	7.62	703	6.70	18.8
5-Nov-19	10DNE	0.12	-	0	0.11	0.1	6.6	7.40	682	0.29	19.5
	8DNE	0.1	0.23	0.1	-	0.9	-	7.35	677	0.17	19.6
	6SNE	0.08	0.05	0.04	-	0.8	-	7.46	698	0.49	19.5
	4DNE	0.02	-	0.1	0.09	0.09	3.4	7.35	637	2.50	19.7
	G30966	0.21	0.29	0.17	-	0.8	-	7.53	689	5.20	19.6
28-Nov-19	10DNE	0.57	-	0.67	-	0.6	-	7.37	644	0.13	19.2
	8DNE	0.98	-	0.44	-	0.4	-	7.62	586	0.11	19.1
	6SNE	0.16	-	0.02	-	0.9	-	7.47	744	0.31	20.2
	4DNE	0.4	-	0.15	-	0.5	-	7.42	638	0.19	19.5
	G30966	0.52		0.14	-	0.4	-	7.52	716	2.35	19.9
2-Dec-19	10DNE	0.02	-	0	-	0.8	-	7.26	712	14.13	19.6
	8DNE	0.24	-	0.46	-	1.0	-	7.20	703	3.46	19.6
	6SNE	0.02	-	0.02	-	0.9	-	7.42	758	0.98	19.5
	4DNE	0.14	-	0.39	-	0.4	-	7.26	691	0.24	19.5
	G30966	0.24	-	0.32	-	0.4	-	7.52	721	1.83	18.9
17-Dec-19	10DNE	0.08	-	0	-	0.3	-	7.35	712	17.89	19.8
	8DNE	0.02	-	0.02	-	0.7	-	7.27	713	19.96	21.2
	6SNE	0.15	-	0	-	0.9	-	7.46	761	0.27	20.3
	4DNE	0.18	-	0.25	-	0.6	-	7.25	670	3.05	19.6
	G30966	0.21	-	0.31	-	0	-	7.54	720	5.66	19.2
21-Jan-20	10DNE	0.05	-	0	-	0.7	-	7.41	716	20.00	20.1
	8DNE	0.02	-	0	-	0.6	-	7.36	719	20.00	20.5
	6SNE	0.08	-	0	-	0.7	-	7.50	657	0.19	19.7
	4DNE	0.13	-	0.2	-	0	-	7.37	667	6.86	19.7
	G30966	0.2	-	0.32	-	1.3	-	7.63	724	5.52	19.1
29-Jan-20	10DNE	0.08	-	0	-	0.4	-	7.46	715	20.00	20.5
	8DNE	0	-	0	-	0.8	-	7.46	715	20.00	20.5
	6SNE	0.03	-	0.01	-	0.6	-	7.62	672	0.20	20.0
	4DNE	0.19	-	0.26	-	0.6	-	7.44	671	5.17	19.8
	G30966	0.21	-	0.39	-	0.5	-	7.54	722	3.49	19.0
5-Feb-20	10DNE	0.03	-	0	-	0.7	-	7.61	717	15.07	19.7
	8DNE	0.03	-	0	-	0.3	-	7.58	717	15.09	19.8
	6SNE	0	-	0	-	0.5	-	7.82	722	7.81	20.2
	4DNE	0.19	-	0.39	-	0	-	7.41	674	2.90	19.5
	G30966	0.19	-	0.41	-	0.3	-	7.58	723	2.74	19.1
12-Feb-20	10DNE	0.11	-	0.21	-	0.6	-	7.54	684	0.30	19.7
	8DNE	0.26	-	0.58	-	0.7	-	7.55	666	0.17	19.4
	6SNE	0.07	-	0	-	1.3	-	7.45	724	7.83	20.4
	4DNE	0.26	-	0.59	-	0.5	-	7.37	677	0.15	19.6
	G30966	0.19	-	0.4	-	0.3	-	7.47	723	2.63	19.8
19-Feb-20	10DNE	0.13	-	0.11	-	1.6	-	7.47	692	0.25	19.8
	8DNE	0.26	-	0.53	-	1.4	-	7.76	669	0.20	19.2
	6SNE	0.03	-	0.03	-	1.1	-	7.37	697	5.00	20.1
	4DNE	0.28	-	0.64	-	1.2	-	7.30	673	0.18	19.2
	G30966	0.21	-	0.45	-	1.4	-	7.48	719	2.38	19.2
26-Feb-20	10DNE	0.03	-	0	-	0.7	-	7.58	712	4.13	19.9
	8DNE	0.02	-	0	-	0.7	-	7.42	713	3.95	20.0
	6SNE	0.03	-	0	-	0.9	-	7.34	690	2.68	20.2
	4DNE	0.2	-	0.43	-	1.7	-	7.34	657	0.62	19.5
	G30966	0.18	-	0.45	-	0.9	-	7.49	718	2.52	19.1
4-Mar-20	10DNE	0.11	-	0.13	-	0.8	-	7.42	686	0.45	19.6
	8DNE	0.21	-	0.42	-	1.3	-	7.47	676	0.25	19.3
	6SNE	0.02	-	0.03	-	0.8	-	7.30	679	2.01	20.1
	4DNE	0.28	-	0.65	-	1.3	-	7.20	687	0.14	19.1
	G30966	0.19	-	0.46	-	0.4	-	7.55	715	5.02	19.3

*Off-site/campus determined results.

Variation in EC (477.4–768) is less than observed for G30966, temperature variation is not significant, and pH is near neutral. It is important to understand the TOC in the aquifer in order to understand how injection at these levels would be affected by the drilling mud. The results for TOC indicate a decline in concentration; from 15.40 mg/L on 29 October, 12.50 mg/L measured for 1 November and 6.60 mg/L for 5 November 2019. The final measurements are within SANS 2015 recommended limits for drinking water. Dissolved oxygen (DO) data range from 0–4.6 mg/L, and the water from the production borehole has DO ranges of 2.2 -5.8 mg/L.

Figure 14 depicts bar graphs for Fe (difference between FeT and FeD), pH, EC and DO compiled from the field data. The graphs indicate the responses of these parameters to the injection treatment. EC and pH appear to be stable in all the boreholes, while DO is highest in 10DNE and 8DNE.

Figure 14. Field parameter data for the pilot site since injection started.

7 CONCEPTUAL GEOCHEMICAL MODELLING

A conceptual geochemical model was developed as a precursor to the quantitative geochemical modelling of the reactions and processes which occur in the aquifer as ozone is injected. The conceptual model describes the reactions which are expected to occur and the impacts they are likely to have on the observed groundwater chemistry.

The aim of ozone injection into the aquifer is to cause a shift in the redox state of the aquifer, resulting in oxidation of Fe^{2+} to Fe^{3+} and precipitation as a ferric hydroxide. Redox reactions follow a predictable sequence based on the energy yielded by the reaction. An oxidant, such as oxygen, entering an aquifer will first oxidise the reductant that will yield the most energy. Only once this reductant has largely been consumed will the next reductant be oxidised. The theoretical sequence of reactions is given in Table 7, along with the expected changes in water chemistry (Appelo and Postma, 1993).

Table 7. Sequence of reactions in an oxidising environment.

Reaction	**Change in aquifer chemistry**
Organic matter oxidized to CO_2	Decrease in organic matter Increase in pCO_2 Decrease in pH due to increase in pCO_2
H_2S or FeS oxidized to sulphate	Increase in sulphate, Decrease in H_2S odour Increase in dissolved Fe^{2+}, Decrease in dissolved oxygen
Fe^{2+} oxidized to Fe^{3+} and precipitation as $Fe(OH)_3$	Decrease in dissolved Fe Possible increase in total Fe (depending on if $Fe(OH)_3$ remains in colloidal form in the aquifer or attaches to the aquifer solids) Decrease in dissolved oxygen
NH_4^+ oxidized to NO_3^-	Increase in NO_3^- Decrease in dissolved oxygen
Mn^{2+} oxidized to Mn^{4+} and precipitation as MnO_2	Decrease in dissolved Mn Decrease in dissolved oxygen

In order to predict the changes in chemistry that will be observed, the baseline oxidation state of the aquifer must be understood. Robey *et al*. (2014) describe the baseline aquifer chemistry at production boreholes G30966 and 10DNE. The baseline concentrations for some of the parameters identified in Table 7 are listed in Table 8.

Table 8. Baseline aquifer parameters for 2014 compared with the current study.

Parameter	Robey *et al*. (2014)		Current study – 1 October 2019	
	G30966	10DNE	G30966	10DNE
pH	7.7	7.5	NA	7.3
DO (mg/L)	0.4	0.4	NA	0.02
FeD (mg/L)	2.24		NA	<0.01
FeT (mg/L)	2.96		NA	0.1

The baseline values collected in 2014 when compared with the current study show some important differences. The DO is lower than had previously been measured, and the dissolved and total iron are far lower than had previously been measured. The water sampled from 10DNE during the baseline test was observed to contain black particulate matter and to have a sulphidic odour. The baseline for the current study is believed to be different to the 2014 study owing to the presence of drilling muds within the aquifer. Organic drilling muds were used during the installation of the new boreholes 11DNE, 7DE and 12DN, and it is believed that the degradation of these drilling muds resulted in more highly reducing conditions in the aquifer than had been the case previously, such that the sulphate reduced to sulphide and precipitated with the iron as iron sulphides, resulting in a low dissolved iron concentrations.

Based on the baseline data, a conceptual model was developed to show the expected changes in chemistry with time (Figure 15). Four time steps are shown:

Time 1 – The ozonated water enters the aquifer. The ozone decomposes in water to form dissolved oxygen and hydroxyl radicals. The hydroxyl radicals have a half-life of microseconds; therefore, the elevated dissolved oxygen concentrations are the main source of oxidation capacity in the groundwater (Robey *et al*., 2014). The DO first reacts with organic carbon present in the aquifer. The aquifer naturally has a dissolved organic carbon content of approximately 9 mg/L, and with the organic carbon present from the drilling muds, this reaction is expected initially to consume all the oxygen.

Time 2 – The dissolved oxygen front is expected to move towards the production well, reacting with organic carbon encountered on the way. If the rate of water flow is greater than the rate of the reaction, dissolved oxygen can move down-gradient before the organic carbon has fully reacted. However, the shift to reacting with iron sulphide minerals is unlikely to occur before a large proportion of the organic carbon has been removed. At time 2, the dissolved oxygen closest to the injection well has started reacting with iron sulphides present in the aquifer, while the organic carbon oxidation zone has moved towards the production hole. As the sulphide in the iron sulphides is oxidised to sulphate, dissolved ferrous iron is released, resulting in an increase in dissolved iron concentration.

Time 3 – As sulphides largely react close to the injection hole, the sulphide oxidation zone shifts towards the production hole, and newly injected dissolved oxygen begins to oxidise ferrous iron to ferric iron. Ferric iron is not stable in near-neutral pH water, and precipitates as iron oxide minerals. The iron oxide minerals could remain as colloids and be transported with the water, in which case they will be measured as total iron, or they could attach to aquifer solids and be immobilised. Regardless, the dissolved iron concentration will decrease. This is the target reaction that will prevent iron from oxidising within the borehole and will therefore limit iron clogging.

Time 4 – Following the complete reaction of organic carbon, iron sulphides and hydrogen sulphide within the aquifer, the predominant reaction expected down-gradient of the injection borehole would be the oxidation of the iron. The only source of iron will be from water flowing in from up-gradient; therefore, iron should be captured within the aquifer in the zone between the injection borehole and the production borehole, and will not be capable of clogging the borehole equipment.

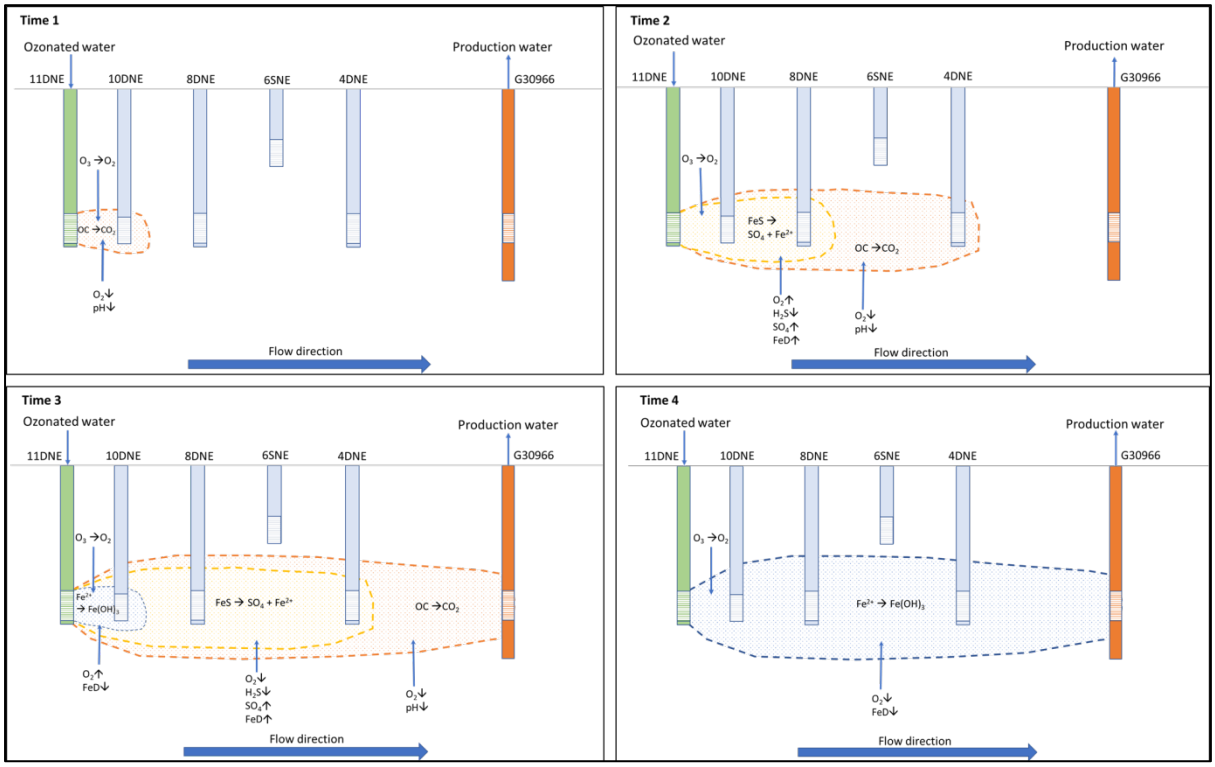

Figure 15. Conceptual geochemical model showing changes over time.

In reality, the segregation of the different oxidation zones is less clear. However, the data collected on-site should provide some indication that oxidation zones are present and that iron oxidation should be achievable. Unfortunately, owing to issues related to injection rates, power outages at the production borehole and various unforeseen incidents, it was not possible to maintain a steady injection rate and, thus, the site data are difficult to interpret.

Graphs of the DO, FeD and FeT data are shown in Figure 16, and some general trends can be observed in line with expected observations:

The DO concentrations fluctuated considerably with time, but concentrations of 18 mg/L and possibly higher were achieved in 10DNE and 8DNE, and DO concentrations were observed to decrease towards the production borehole.

Dissolved iron concentrations also showed great fluctuation in each borehole over time, but concentrations below the detection limits are observed on several occasions in 10DNE and 8DNE, whereas concentrations in 4DNE and the production hole appear to be generally increasing, possibly as a result of the oxidation of iron sulphides releasing ferrous iron.

Total Fe concentrations were lower in 10DNE and 8DNE than 4DNE and G30966. However, there is some question as to the reliability of the total iron concentrations as many are lower than the dissolved iron concentrations, particularly in 4DNE and G30966.

Figure 16. Trends in DO, FeD and FeT with time in boreholes between the injection borehole and the production borehole.

8 ENGINEERING DESIGNS

The project requirements were for the design and construction of a secure and automated system for injecting ozonated water into three separate injection boreholes.

The brief included the following requirements:

- Use the experience and knowledge gained from the previous project.
- Design the infrastructure to test long-term continuous injection of ozonated water.
- The installation must be secure and not need on-site security.
- The design should make use of as many of the available existing components as possible.
- The design must allow flexibility to accommodate changes to allow for the testing of different variables.
- The design must enable the monitoring of water chemistry, flow rates and borehole water levels.
- The infrastructure must be designed such that it can be moved to other test sites but so that it can also be utilised for permanent installations.

The design consists of the following elements:

- A side stream of abstracted groundwater is tapped off from the pipework at the wellhead of G30966 and piped to below ground level to a containerised treatment facility.
- Inside the shipping container, water is first aerated and then stored in a 5 000 L plastic tank.
- The injection water is pumped from the storage tank, dosed with ozone and distributed to three injection boreholes, 12DN, 11DNE and 7DE.
- Monitoring of water levels, chemistry and flow rates is done at several key points in the system.

The system flow was designed to operate as follows (Appendix B):

Source water is drawn from a side stream of the delivery pipework from abstraction borehole G30966 and is delivered to the containerised system at a flow rate of 1.5 L/s. The volume of water delivered is measured though a 40 mm water meter installed downstream of a 50 mm globe valve that can be used to throttle flow to the required flow rate. From the globe valve, water passes through a venturi that is connected to an ozone generator without an oxygen generator. The pre-storage ozonation is to allow for iron in the ground water to oxidise and precipitate out of the water during storage and to collect at the bottom of the storage tank. The ozonated water then enters the storage tank through a mechanical float valve, which will close the flow into the tank automatically when the tank is full.

The outlet from the tank is raised 1 m from the bottom of the tank to allow space for the accumulation of iron that precipitates out of the groundwater. The tank is also installed with a scour or washout valve that can be opened to flush out the iron that accumulates at the bottom of the tank.

Water is pumped out of the storage tank with two (2) JA 100 Foras pumps installed in parallel. One of the pumps can deliver half the possible required flow, with both pumps being able to deliver the full 1.5 L/s. The water is pumped through two venturis in parallel. Each venturi is connected to an ozone generator with oxygen generator. The ozonated water then passes through a degas column where excess ozone is vented out of the system through a degas valve. The excess ozone vented through the degas valve is fed to the incoming pipework to aid in the oxidation of Fe in the source water.

After the degas column, the water is split into three (3) streams, each monitored by means of a water meter to measure volume of water injected and a globe valve for adjusting the flow rate to each injection borehole. After the globe valves, water is fed through 50 mm pipework to the three injection boreholes, 12DN, 11DNE and 7DE.

A sample tap was installed on the inlet pipe work before the storage tank to sample the water before any ozonation. Another sample point was installed after the degas column, to sample the water after ozonation and before injection.

Two sampling point columns were installed for continuous inline DO monitoring. One is for the source water and the other for sampling the ozonated injectant water.

The operation considerations for the system involve the following:

The system is designed for a full flow of 1.5 L/s. The flow can be adjusted by means of the globe valve on the incoming pipework and by measuring the flow through the incoming water meter.

The flow to each injection borehole is controlled by adjusting the globe valve on the pipework to each borehole and by measuring the flow through the water meters for each borehole.

If the combined flow required to the injection borehole is more than 0.75 L/s both booster pumps should be in operation. When both pumps are in operation the flow should pass through both venturis installed in parallel.

When the combined flow to the injection boreholes is less than 0.75 L/s, one pump should be taken out of operation by switching off the power to that pump at the control box and by isolating the pump that has been taken out of operation by closing the gate valve between the storage tank and the pump. Venturi 1078 (the bigger of the two) should then also be isolated by closing the gate valve before and after the venturi so that all the flow will pass through (the smaller) venturi 784.

Every time the flow rates to the injection boreholes are adjusted, the combined flow rate must be summed to determine whether one or two pumps are required and to determine whether one or both venturis should be used.

9 TELEMETRY SYSTEM

The science of collecting data from a source point based far away, and sending the information somewhere else electronically is known as telemetry. There are three types of telemetry systems in existence, namely: frequency, position and multiplexing. Sensors that measure physical properties such as temperature, pressure or pressure at the source area form a data stream that is transmitted over a wireless, wired or combination medium (Aziz and Hussein, 2009).

The advantages of using a telemetry system include the following:

- Telemetry provides an efficient and convenient method of collecting remote data.
- Less time and money are spent traveling to the site, and there are cost savings (without the inclusion of data hosting fees).

The company GeoTel Systems was appointed to install a telemetry system for this project. A wireless medium was used to connect a number of remotely located data loggers to a cloud-based database (from a telemetry box located within the treatment plant on-site), for viewing continuous, real-time data. The data is accessed through the GeoTel website through a log-in system where data are viewed through display graphs, and downloaded into a Microsoft Excel spreadsheet. Figure 17 presents a schematic diagram of the telemetry system at the pilot site (the remote location) and the data flow.

A total of six (6) data loggers were installed for remote monitoring into the injection boreholes, two monitoring boreholes and the internal/aeration tank. In order to avoid data clogging, monitoring frequency in the data loggers was set to an hourly frequency. The dissolved oxygen (DO) loggers were supplied by Global Water (an American company), and these were installed in BH8DNE and the internal/aeration tank. The rest of the data loggers were supplied by Solinst and measured water level, temperature, conductivity and injection flow rate (Figure 18).

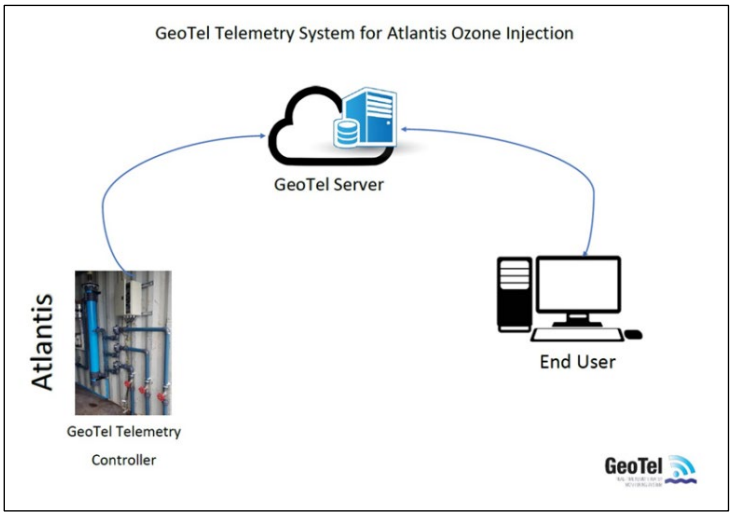

Figure 17. Schematic representation of a telemetry set-up.

The Solinst data loggers have an internal battery, and data can be manually downloaded from them during a power failure to the telemetry system (obviating a loss of data). The data loggers are robust and can be used in harsh (corrosive) conditions. The models used in this project (F100, M30) have a submergence depth of up to 100 m. The Global Water WQ-FDO sensor and GL500-7-2 data logger exist on the DO logger. The data output of this logger is proportional to oxygen partial pressure, and water temperature. The partial pressure is recalculated to give DO measurements in mg/L using the equation:

$$C = PPO_2 \times [(6.906334E^{-2}) - (1.797779E^{-3} \times t) + (3.108257E^{-5} \times t^2) - (2.199777E^{-7} \times t^3)] \quad (4)$$

Where C = concentration of do in mg/L, PPO_2 = measured oxygen partial pressure in mbar and t = measured water temperature in °C.

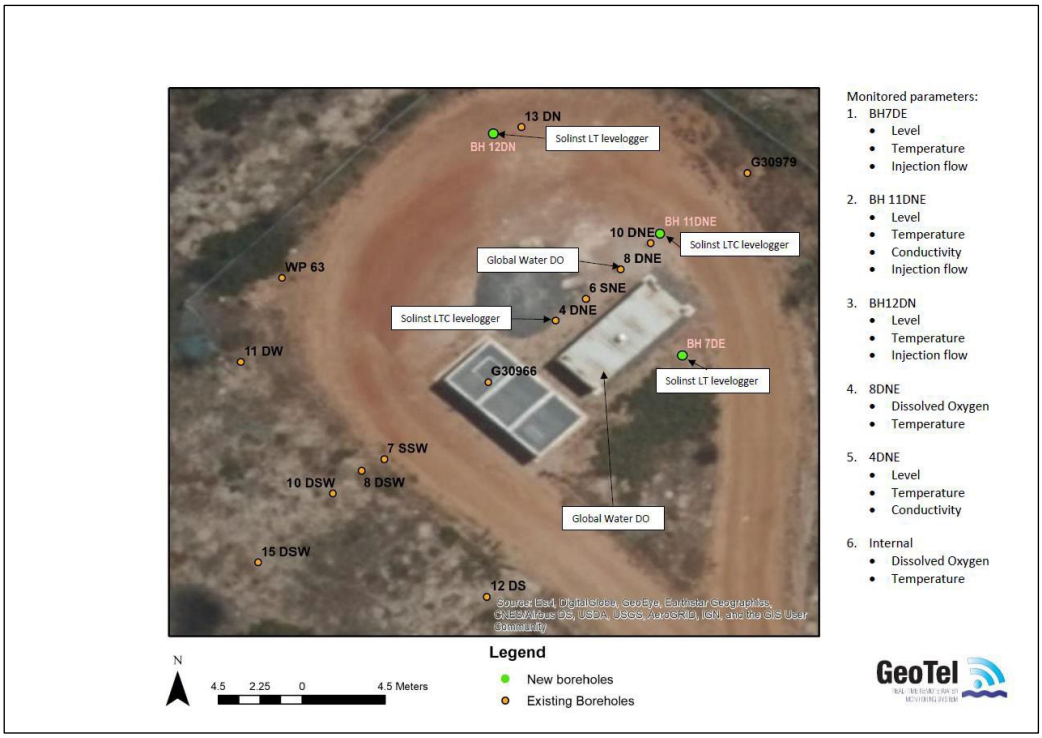

Figure 18. Location and description of data loggers feeding the telemetry system.

Although the data are transmitted wirelessly, on-site the different data loggers have been lowered to 25m depth in the boreholes via direct read electrical wires, and are fed to the telemetry box which is powered by electricity. The telemetry box has the dimensions of (39.5 cm x 30 cm x 20 cm) and houses the essential components (Figure 19). The telemetry is not required for day-to-day operation and is therefore locked for security reasons, and only checked for power flow status (at the power box).

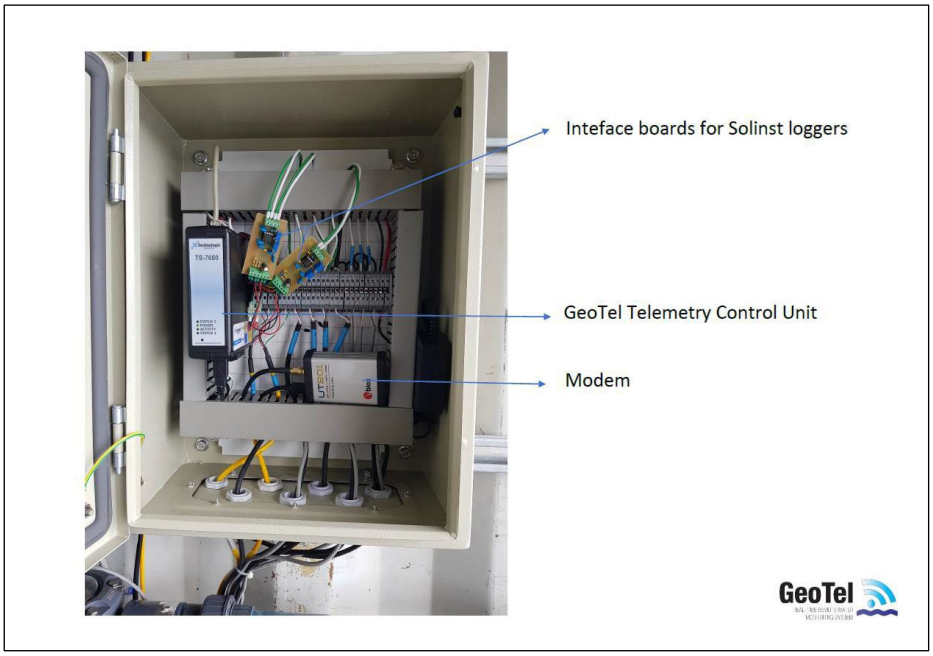

Figure 19. Operational components of the GeoTel telemetry box.

10 TREATMENT PLANT OPERATION AND RESULTS

As an upgrade to the injection system from the first pilot project (Robey, 2014), engineering designs were drawn up to optimise the system. The treatment plant was assembled as per the engineering blueprints, and commissioned in October 2019. However, this is an on-going process, as adjustments and modifications to the fitting are made when problems arise, and to suit different injection configurations.

The treatment plant is mobile ready and can be uprooted to a different location. The plant is now housed inside a shipping container, instead of a caravan. The treatment system has been designed to be able to run un-manned (around the clock; 24/7) and automated.

A used steel general-purpose shipping container measuring about 5.9 m in length, 2.3 m in height and 2.3 m in width was procured. A gravel basement platform was constructed on which the container rests, and a whirly bird was fitted on the roof to improve ventilation inside the container. The floor of the container was painted with a black rubber paint to ensure improved grip, especially when wet (Figure 20).

Figure 20. Treatment plant and shipping container, installed next to the production borehole.

Trenches were dug and pipework was laid down, connecting the newly drilled boreholes — the two selected monitoring boreholes and ve treatment plant. Vandalism is a serious concern in Atlantis; as a result, the treatment plant and the newly drilled borehole had to be

secured. Heavy cement manholes were fitted on top of the injection boreholes and the two monitoring boreholes were fitted with data loggers (Figure 21).

Figure 21. Positions of monitoring and injection boreholes fitted with manholes (A) and a look inside one of the injection boreholes (B).

Before pipework commenced the condition of the shipping container (treatment plant) was assessed. It was found that the plant required costly repair work that could delay the programme. In order to allow for better roof drainage during the rainy season, it was decided to lift the container on one site, and to continue with the project.

Figure 22. View inside the treatment plant and the collection ofprocessing equipment.

The automation of the treatment involves different data loggers that were installed in the injection boreholes, monitoring boreholes and the water tank inside the treatment container. These were connected to the telemetry system, installed inside the treatment container, and the data were then stored off-site (GeoTel servers) and in the cloud. The data can be viewed and downloaded remotely through an access-regulated website.

Telemetry data for the monitoring boreholes, injection boreholes and the raw water from G30966 (depicted as internal monitoring) are indicated in Figure 23 to Figure 28 and the data loggers were installed in each borehole. Viewing the data off-site served as an early warning system. For example, during the December 2019 holiday season, there was power failure in the area, and the system shut down for about two weeks.

Interruptions in monitoring, mostly attributed to power failure, are seen where the data are erratic (especially in regard to DO, temperature and conductivity). Water level graphs indicate the start of injection into the systems, together with temperature. In the injection and monitoring boreholes, the red line (seen in the water level graphs for BH12DN, BH7DE and BH4DNE) indicated a depth limit for the data.

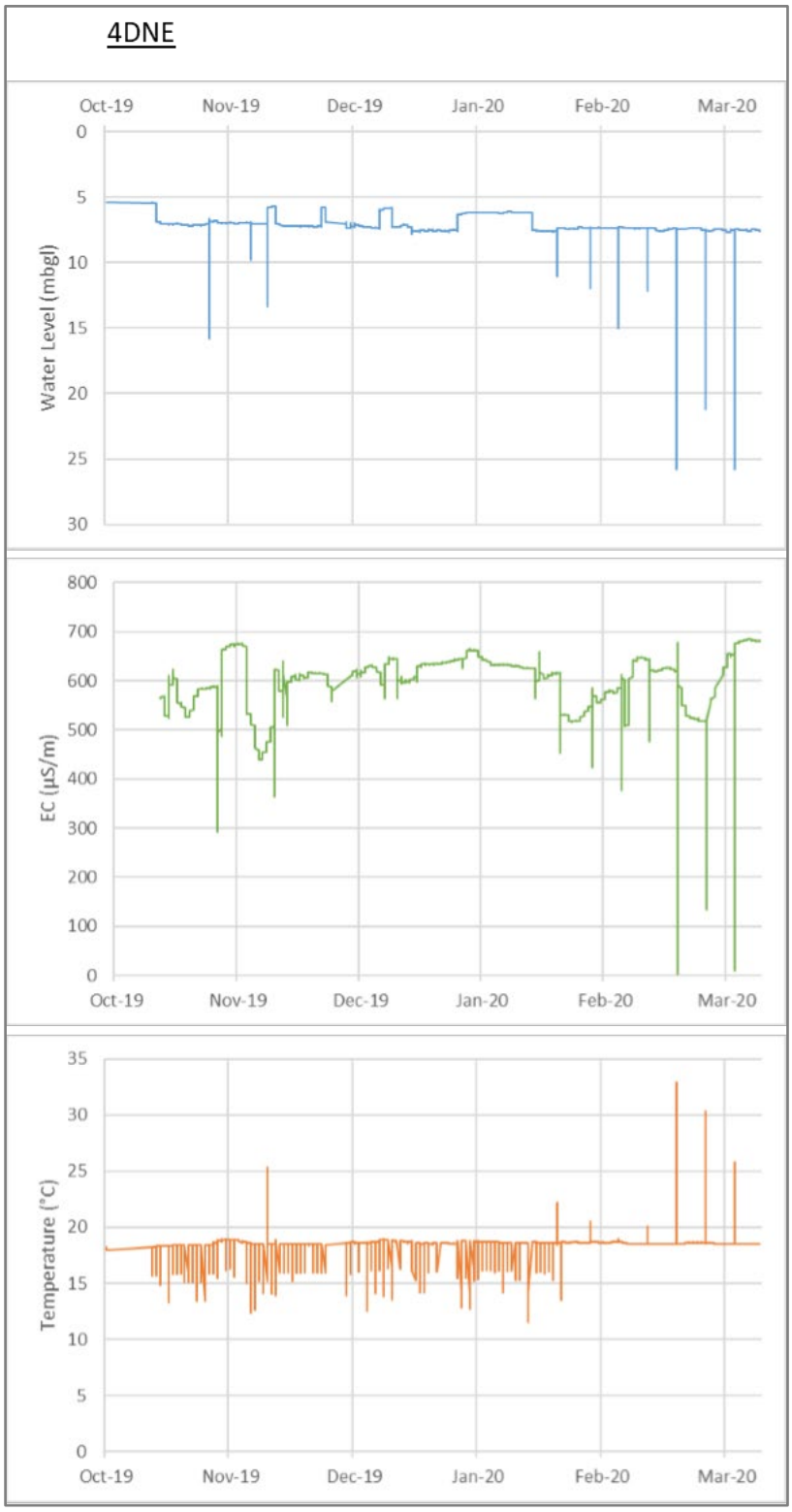

Figure 23. Captured telemetry captured data for monitoring borehole 4DNE to date.

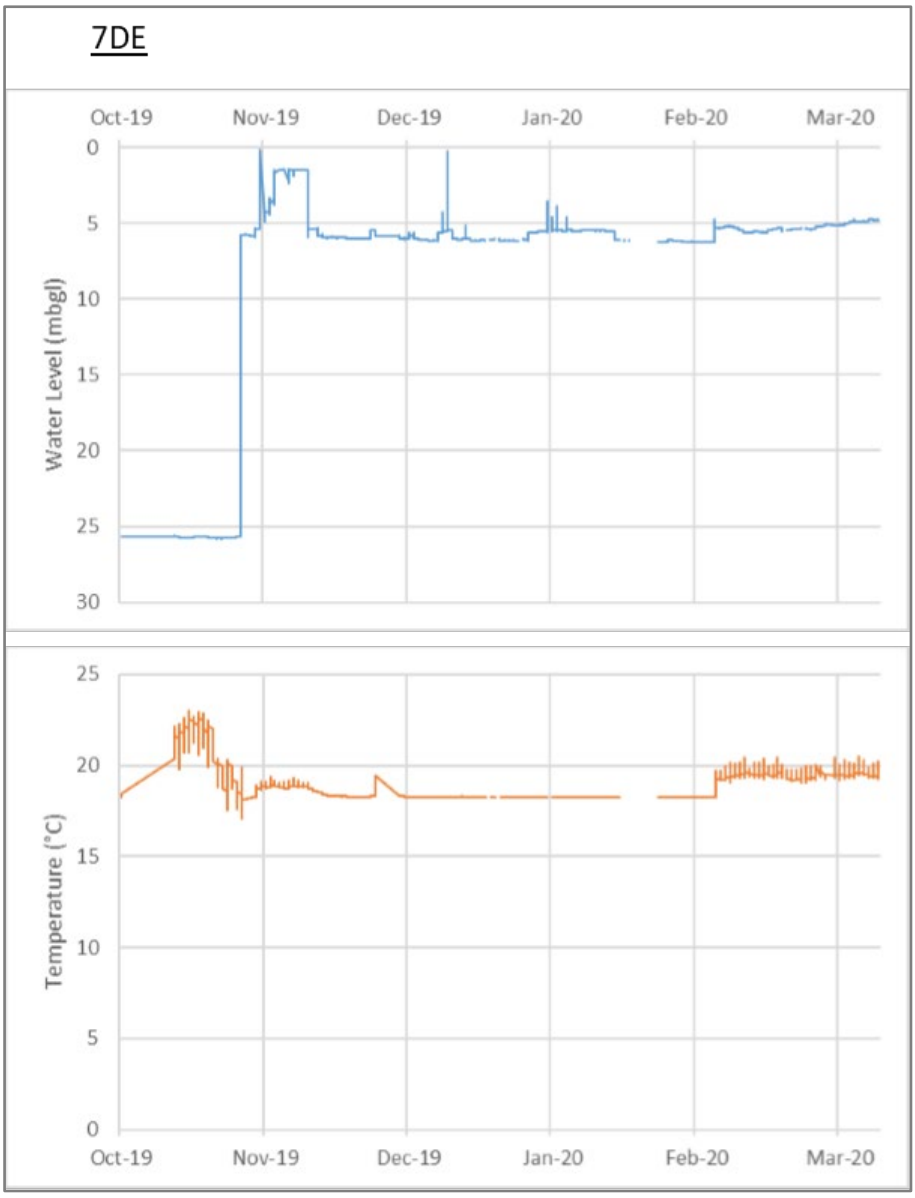

Figure 24. Captured telemetry data for injection borehole 7DE to date.

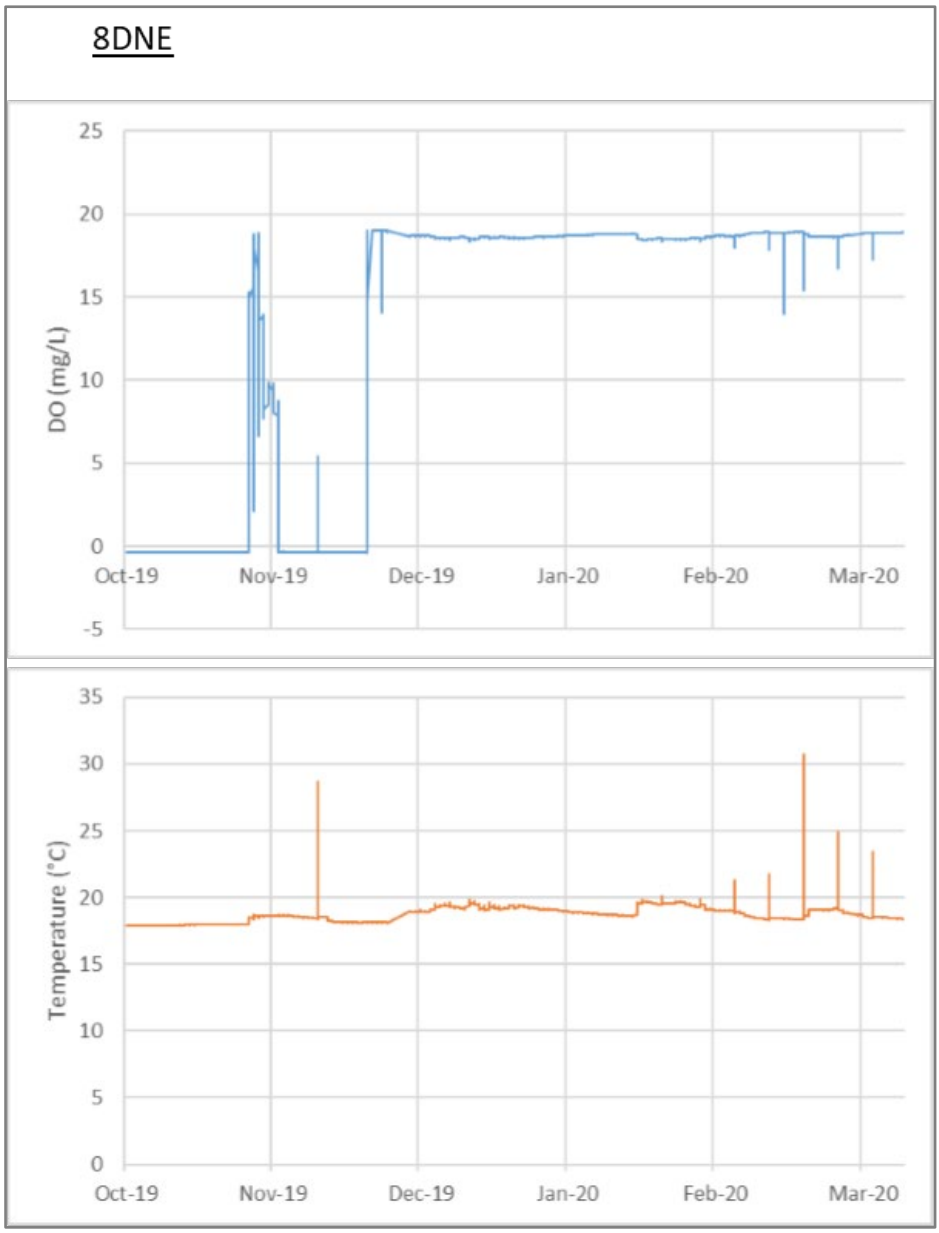

Figure 25. Captured telemetry data for monitoring borehole 8DNE to date.

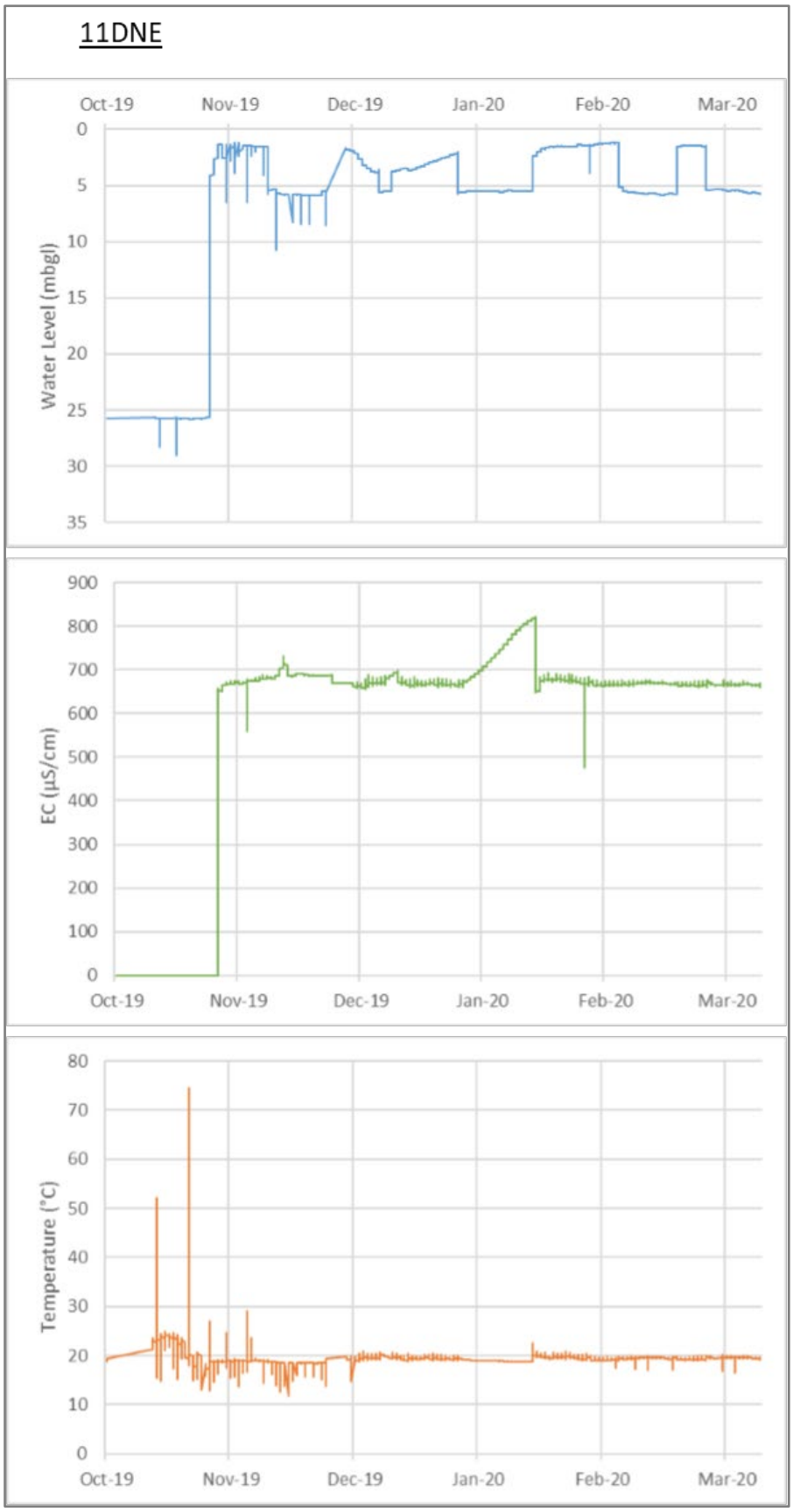

Figure 26. Captured telemetry data for injection borehole 11DNE to date.

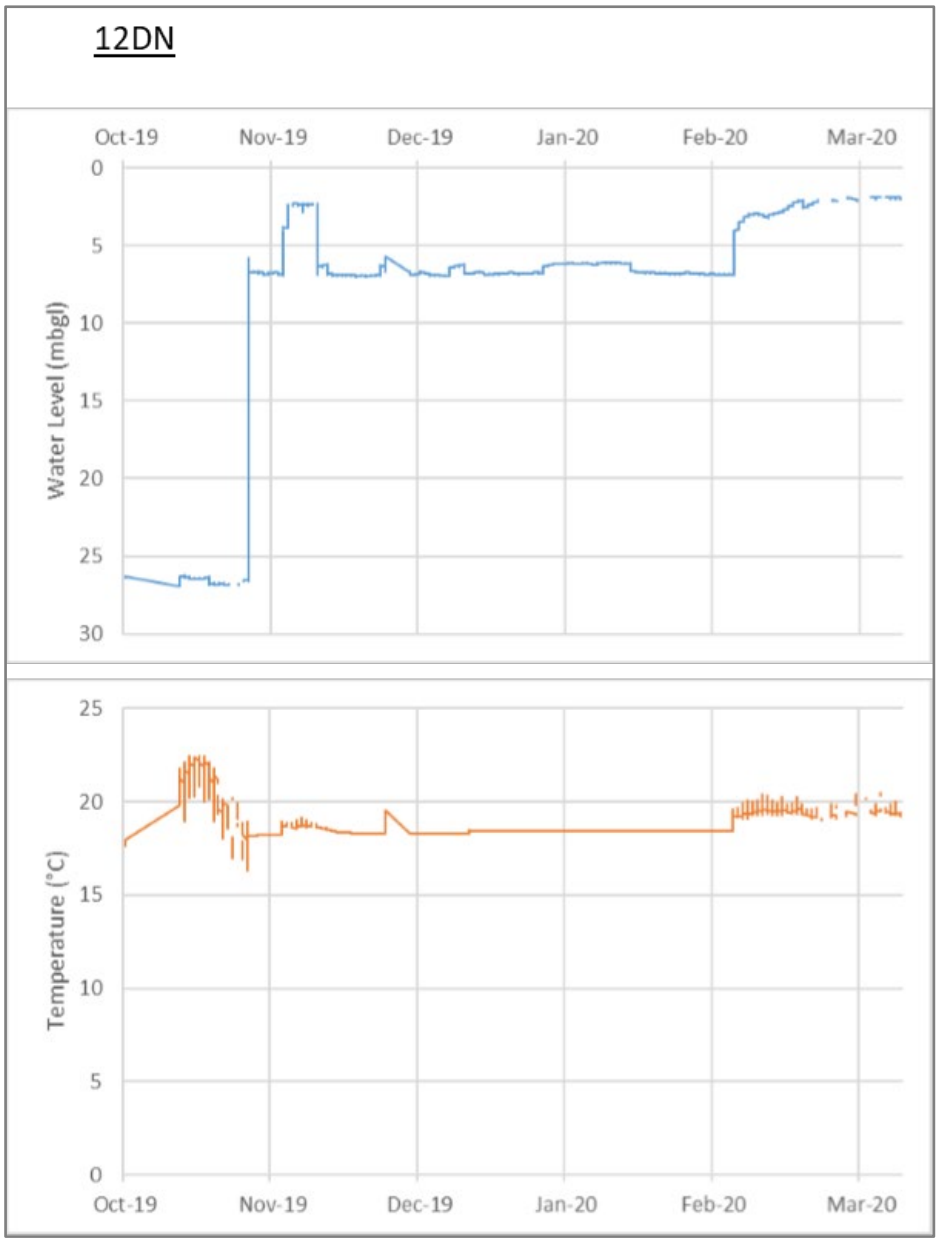

Figure 27. Captured telemetry data for injection borehole 12DN to date.

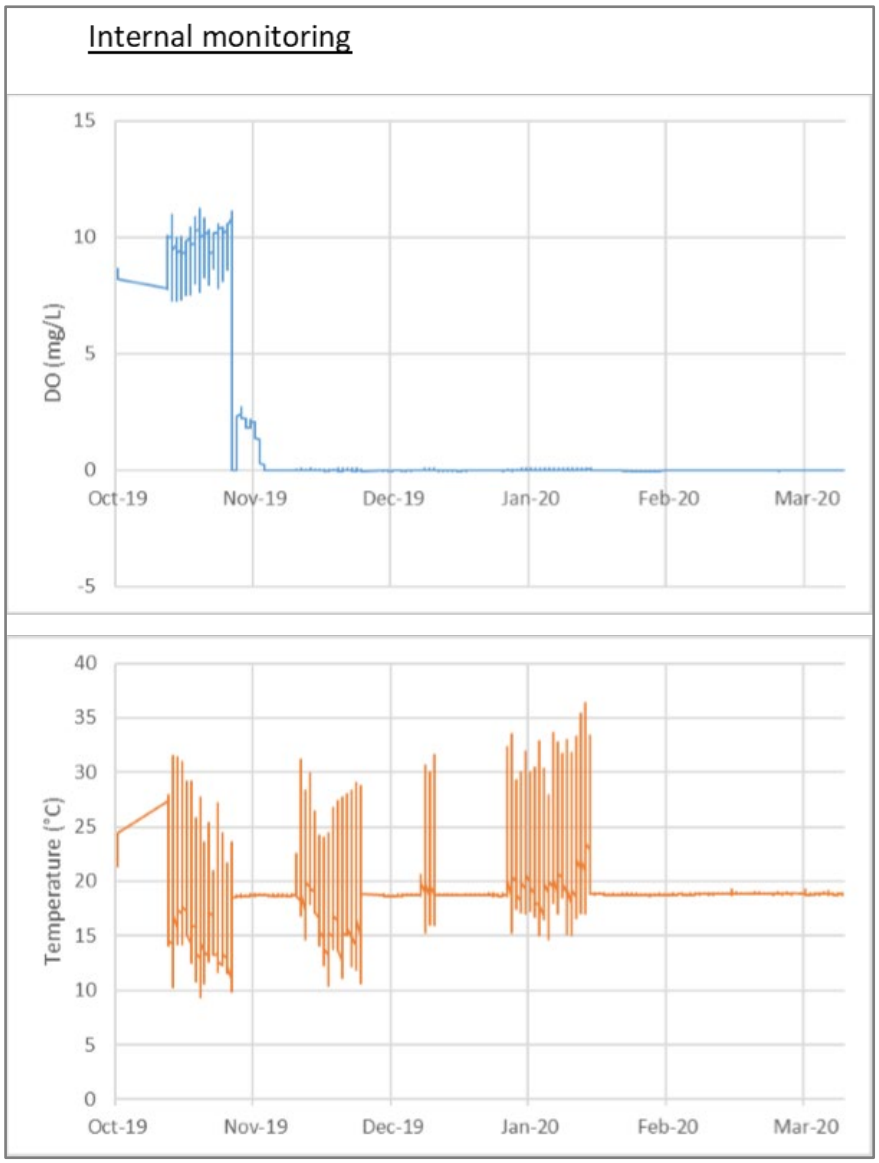

Figure 28. Captured telemetry data for G30966 located inside the treatment plant (prior to entering the water tank).

Overall, the telemetry monitoring works well, but some questions remain with respect to the DO probes. The manual DO measurements were compared with those via telemetry and the results for borehole 8DNE are shown in Figure 29. Although there is some agreement in the overall pattern, the exact times and concentrations do not correspond. In addition, when injection rates were changed and ozonation was discontinued on 19 February 2020 owing to an ozone generator malfunction, the telemetry data did not register any response.

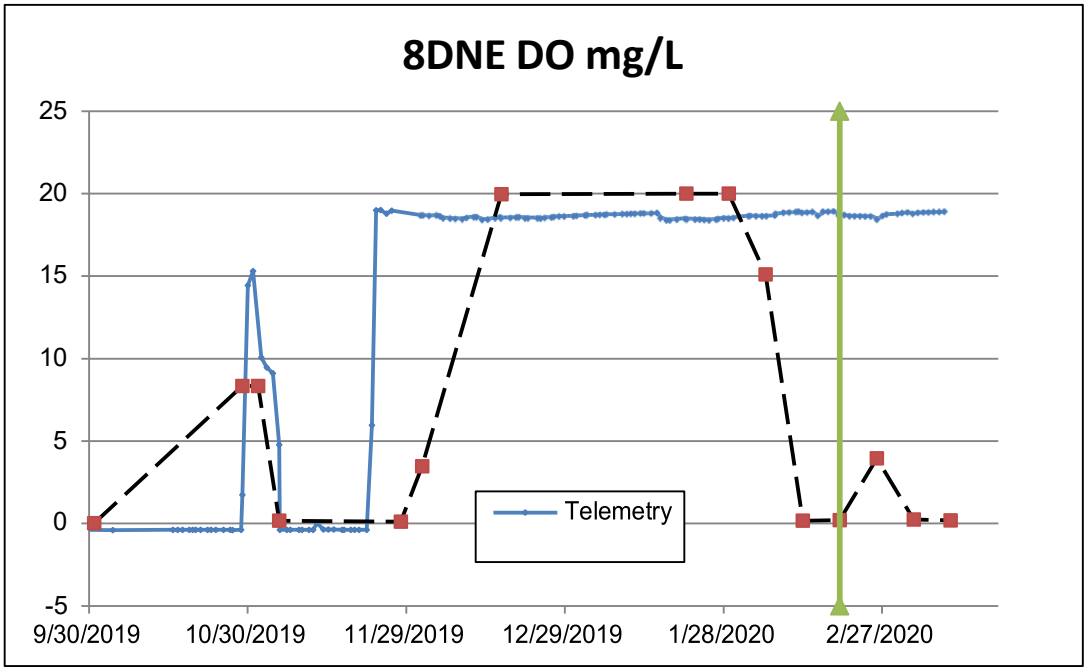

Figure 29. Comparison of DO readings recorded telemetrically with manual DO at monitoring borehole 8DNE.

The DO concentration in the raw water abstracted from borehole G30966, before degassing and ozonation, is a key parameter in the development of the *in-situ* treatment process and real-time monitoring is considered essential. For unknown reasons, the DO probe was dysfunctional as it provided a DO reading of zero most of the time (Figure 30). The manual measurements indicated that the ozone/oxygen injection rate was high enough to reach the production borehole, as untreated groundwater had a DO reading in the order of 0.2 mg/L (Robey *et al*., 2014).

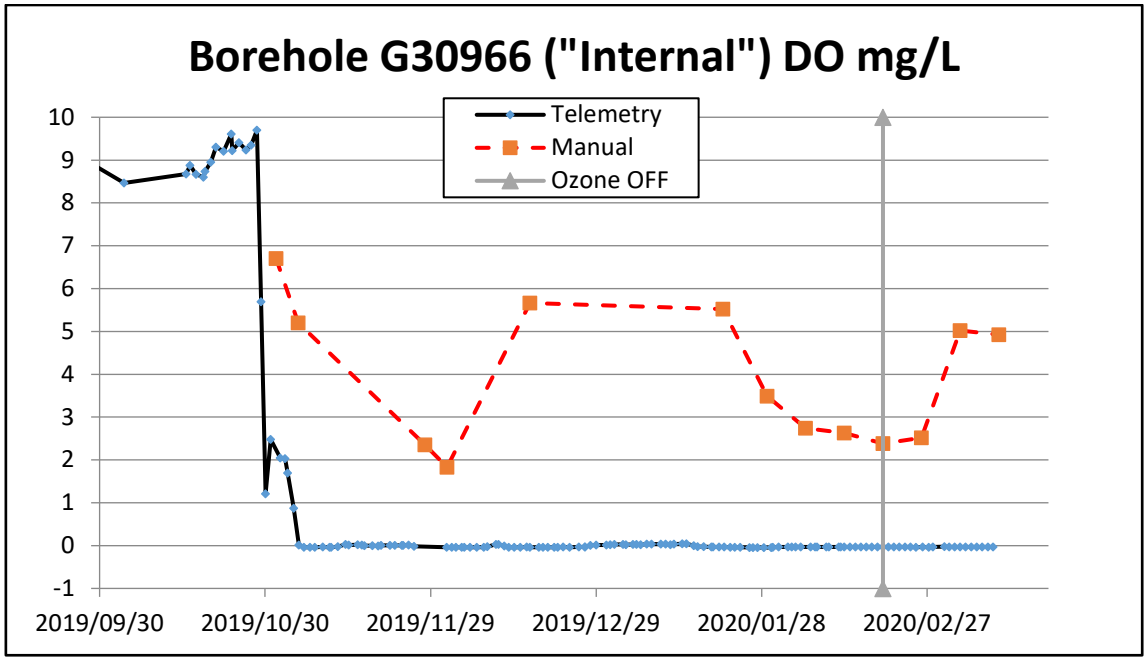

Figure 30. Comparison of DO readings recorded telemetrically with manual DO measurements of the raw water in production borehole G30966.

The accurate determination of total Fe and dissolved Fe requires a dedicated approach as there are numerous factors that affect the concentration of these species. Possibly the most important factor is the extent of the purging of the borehole (Robey *et al*., 2014). Owing to budgetary constraints, Fe analyses were done in the field with no laboratory back-up, which increased the uncertainty of the results. The total Fe determination from December 2019 onwards yielded consistent results and it is considered significant that the total Fe at the production borehole G30966 remained at approximately 0.2 mg/L (Figure 31). Even down-gradient of the production borehole at 8DSW, the total Fe concentration remained at this level. At monitoring boreholes 10DNE and 8DNE, located closer to the injection borehole, the DO concentration was higher and the Fe concentration lower until the ozonation was discontinued.

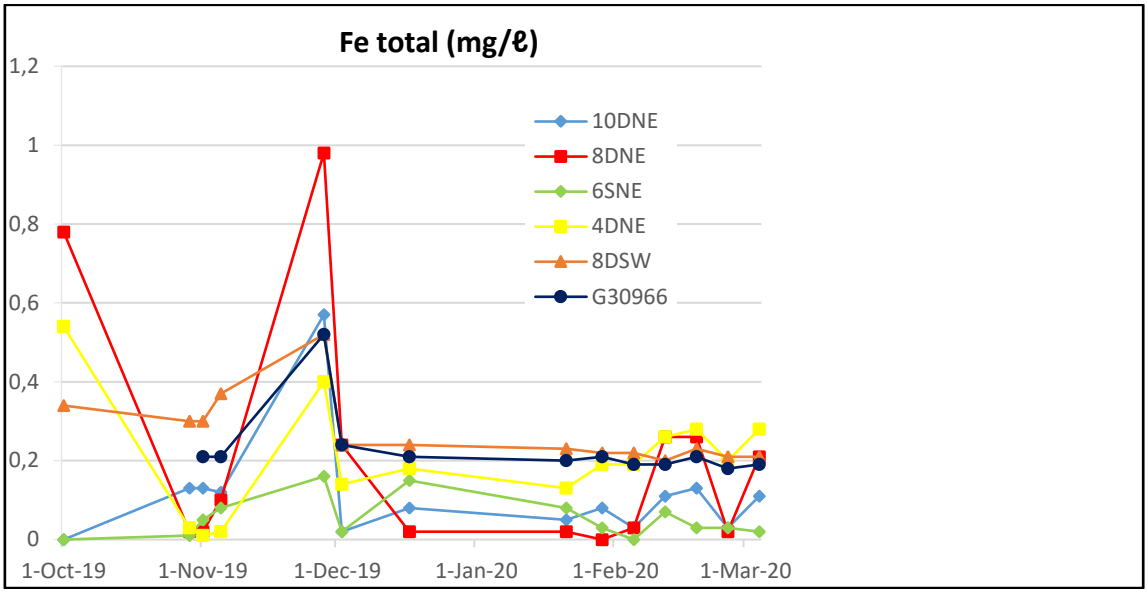

Figure 31. Total iron concentration in the production borehole and several monitoring boreholes during ozonation.

Within the first few days after ozonation had started, a small set of fairly consistent results was available (Figure 32). At monitoring borehole 10DNE, the closest to injection borehole 11DNE, the dissolved Fe was virtually zero while total Fe was just >0.1 mg/L. At 4DNE, close to the production borehole, both total and dissolved Fe (albeit inconsistently) were close to zero. Down-gradient of the production borehole, at 8DSW, dissolved Fe was <0.2 mg/L and total Fe <0.4 mg/L.

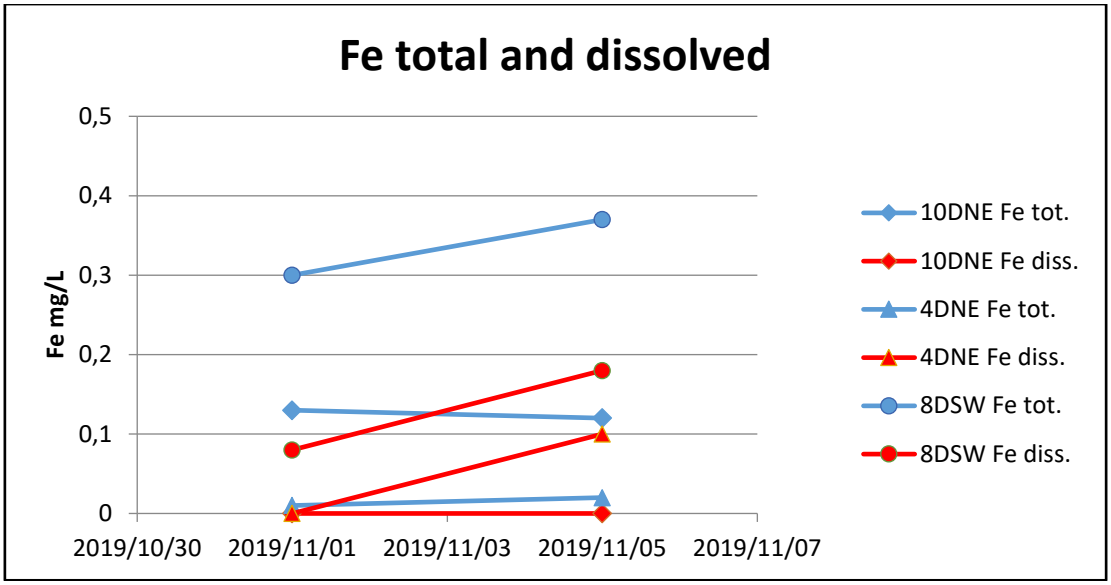

Figure 32. Fe concentrations at observation boreholes in the first days after ozonation had commenced.

The field determinations of Mn yielded very erratic results and it is difficult if not impossible to draw any conclusions from these analytical results. However, just after commencement of ozonation two sets of samples were submitted for laboratory analysis and these results are shown in Figure 33. In most cases, the total and dissolved Mn concentrations were generally the same for a particular monitoring point. At the up-gradient monitoring boreholes 10DNE and 4DNE, the Mn concentrations were approximately 0.1 mg/L while at the down-gradient borehole 8DSW, the Mn concentration was 0.2 mg/L. These data agree with earlier measurements by Robey *et al*. (2014).

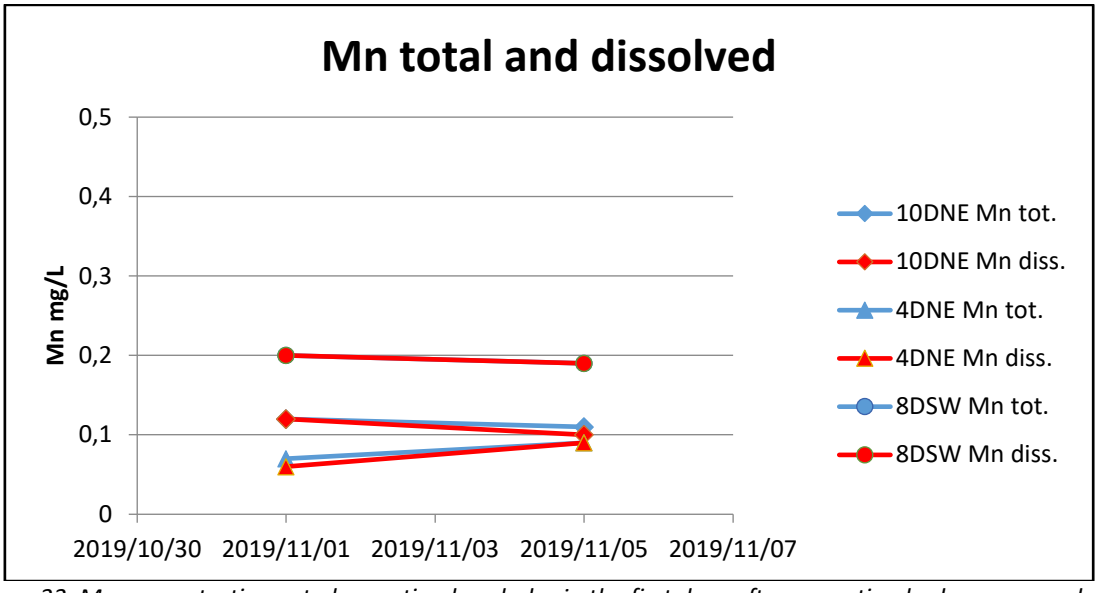

Figure 33. Mn concentrations at observation boreholes in the first days after ozonation had commenced.

11 DISCUSSION

The project was planned to investigate the potential risk of clogging the aquifer matrix owing to the precipitation of iron oxides during *ISIR* treatment. This study was to be achieved by analysing undisturbed core samples of the aquifer material obtained via a suitable drilling technique before and after the *in-situ* treatment test period. In addition, the automation of most components of the system for testing of the ozone treatment necessitated drilling larger diameter injection boreholes as the existing boreholes could not accommodate all the equipment.

Given that the drilling services procurement did not specify the drilling technique, mud-rotary drilling was applied. This drilling technique cannot provide undisturbed core samples and the sampling of the aquifer material had to be abandoned. In addition, the drilling of the three injection boreholes was riddled with difficulties, which necessitated re-drilling the holes and, in the process, large quantities of the organic drilling mud were used with a significant portion remaining in the aquifer. The presence of this material was confirmed after the drilling when the first groundwater samples were taken at the nearby observation boreholes (Figure 34).

Figure 34. Black water observed during sampling, caused by the drilling of mud residue.

On 7 August 2019, a step-drawdown test was performed on production borehole G30966. The drawdown was monitored at observation boreholes 10DNE and 10DSW. Although there was some difficulty in determining the correct pumping rate, the responses at 10DSW for

the four steps are clearly distinguishable. However, borehole 10DNE showed a sluggish response.

At the beginning of September 2019, when the extent of the drilling mud in the aquifer became apparent during sampling, the injection boreholes were pumped to remove as much of the organic material as possible. As the drilling mud is composed of organic compounds, it was expected to interfere with the oxidation of Fe and Mn, and would also impede groundwater flow due to its high viscosity. Two months later, the level of organic carbon, mostly related to the drilling mud, was still high. Table 9 indicates a significant decrease in TOC at the well screen depth due to the injection of high concentrations of ozone and oxygen. However, it is postulated that a significant quantity of the drilling mud is still lodged in the aquifer matrix, particularly above and below the screen depth where groundwater movement is expected to be minimal. Groundwater flow is enhanced at the screen depth where coarser sand occurs. The screen depth is the same for the production borehole, all the injection boreholes, and the deep observation boreholes.

The ozone was injected at this depth interval via the injection wells as this would contribute to oxidation of the organic drilling mud in that part of the aquifer, as well as at least part of the natural organic matter.

Table 9. Reduction in TOC with time in the monitoring boreholes.

Date	10DNE	4DNE	8DSW
2019-10-29	15.4	15.7	5.1
2019-11-01	12.5	3	4.9
2019-11-05	6.6	3.4	4.2

Borehole G30979, a few metres up-gradient of injection borehole 11DNE, possibly filled up with drilling mud during the installation of the new injection boreholes. This was discovered when sampling commenced and on 21 August 2019. The driller returned to site to pump out the borehole. Several of the monitoring boreholes, especially 10DNE, showed pollution with the viscous drilling mud in various stages of decomposition. Comments were made in the field tables regarding the black “sulphidic” water from the monitoring boreholes, especially at the end of October 2019. In an attempt to remove as much as possible of the drilling mud from the aquifer, the three injection boreholes were pumped for several hours on 26 September 2019.

The new ozone generator has a considerably higher yield, which ensures a higher gas concentration in the subsurface. This led to high concentrations of dissolved oxygen (DO) up to approximately 20 mg/L (or possibly even more) in the groundwater at observation boreholes 10DNE and 8DNE. At 4DNE, the DO reached nearly 13 mg/L at an early stage. However, at these high levels, gas bubble clogging of the sandy aquifer is a major possibility and will happen when the gas concentration exceeds the solubility of oxygen and ozone under ambient temperature and pressure in the aquifer. The presence of significant quantities of the organic drilling mud possibly worsened the problem as this material caused

foaming which was observed at the injection boreholes. The foam possibly stabilised the bubbles in the aquifer, aggravating the clogging. The only way to solve this problem is to keep pumping the production borehole while injecting gas-free water while perhaps even increasing the pumping rate. Performing a further step-drawdown pump- test should assist in assessing the extent of the clogging and determining whether there was any subsequent reduction in the clogging.

Owing to inadequate funding, the analytical data consist essentially of field measurements and analyses with very few laboratory results. This has affected the quality of analytical data and has led to discrepancies in the values of total and dissolved Fe that could not be resolved. This has made the interpretation of ozonation results impossible.

Mn field analyses were even more compromised but, in this case, laboratory results were available to confirm that the results were erratic. The laboratory results were comparable to analytical results from the earlier project (Robey *et al*., 2014).

The field analyses of DO provided a useful input to the understanding of the processes. However, complications introduced by the organic drilling mud seriously hampered the interpretation of the data.

Conceptual geochemical modelling was included as the actual modelling still needs to be carried out. Insufficient consistent analytical data was available for this purpose. The write-up explains which factors and redox couples need to be taken into account for the modelling.

Table 10. Timeline of actions carried out on-site.

Date	Abstraction	Injection			Notes
	G30966	7DE	11DNE	12DN	
2019-05-23					Drilling of injection boreholes
2019-08-08					Step test pumping of G30966 showing clogging of aquifer towards 10DNE
2019-08-21					Pumping out of G30979
2019-09-04					Pipework removed and cover plates cut for easy access
2019-09-26					Pumping from all injection boreholes to remove as much drilling mud as possible
2019-10-01					Baseline sampling
2019-10-16	5.37				Start of weeklong pumping of borehole G30966: RWL-4.55
2019-10-29		0.2	1.7	0	***Ozone injection started***
2019-11-01	4.7	0.2	1	0.3	Sampling
2019-11-05		0.7	0.5	0.4	11DNE overflowing - new injection rates
2019-11-28	5.43	0.7	0.5	0.4	G30966 restarted after power cut
2019-12-02		0.7	0.5	0.4	Sampling
2019-12-17		0.7	0.5	0.4	11DNE foam on surface of WL probe (due to injection)

2020-01-15		0.7	0.43	0.4	G30966 off due to power outages
2020-01-21	5.13	0.7	0.43	0.4	11DNE foaming - ozonation resumed - WL reading could not be taken
2020-01-29	5.06	0.7	0.43	0.4	11DNE still foaming - flushed out with water
2020-02-05	4.9	0.44	0.1	0.38	11DNE overflowing - new injection rates
2020-02-12	4.8	0.27	Negligible	0.46	7DE starts foaming - injection rates adjusted
2020-02-19	4.9	0.27	Negligible	0.46	***Ozone generators switched off - injection continues***
2020-02-26	5.14	0.27	Negligible	0.46	11DNE overflowing
2020-03-04	5	0.27	Negligible	0.46	Ozone generator is still off
2020-03-11	5.2	0.27	Negligible	0.58	Ozone generator is still off

Table 10 lists the timeline of actions at the field site at production borehole G30966. Drilling of the new injection holes with a larger diameter using the mud-rotary technique necessitated the establishment of a large drill rig on-site and the digging of large holes for mud circulation. These activities had a vast impact on the site especially owing to the use of the drilling mud and the re-drilling of the northern injection hole after the initial one had collapsed. Thus far, no drilling report has been made available.

12 CONCLUSIONS

The mechanisation of a significant part of the field-testing setup allowed for hourly recording of several key parameters such as the water level, temperature and EC at several boreholes, as well as the injection rates in the three boreholes, and the dissolved oxygen concentration at two points. Using telemetry, the data was accessible in real time. This set-up indicated that remote monitoring through system automation and the use of telemetry is effective in reducing manpower and travel costs.

The field-testing was partially successful as several local and external factors interrupted the smooth operation of the abstraction, injection and recording system, such as load shedding. Local factors included the malfunctioning of the venturis, the venturi-pump relationship, operation of the new ozone generator, and other teething problems.

The presence of drilling mud was a serious obstacle. The step drawdown test on production borehole G30966 identified a sluggish response in the direction of the injection borehole 11DNE (that was not caught during this time). This is probably due to gas bubble clogging of the aquifer affecting the aquifer near the injection borehole(s). The presence of significant quantities of drilling mud and the high concentration of gas in the injected water are probable causes. The high concentration of oxygen and ozone exceeds the solubility of oxygen and/or ozone at the ambient temperature and pressure in the aquifer.

Over most of the field test period the total iron concentration at the up-gradient monitoring boreholes and the production borehole was approximately 0.2 mg/L, which is lower than the baseline value of 0.5 to 0.8 mg/L. At borehole 8DSW situated 8 m down gradient of the production boreholes the total Fe concentration varied between 0.3 and 0.4 mg/L. This is a clear indication of reduced iron concentrations in the aquifer as a result of the ozonation treatment, and the effectiveness of this technology at injection distance of 10m from the production borehole.

The manganese field test did not seem to yield correct results but laboratory analyses of samples taken at the beginning of November 2019, after ozonation started, consistently gave concentrations of approximately 0.1 mg/L for both total and dissolved manganese. Down gradient of the production borehole total Mn registered 0.2 mg/L, to within the maximum allowed concentrations as set out by SANS 241: 2015 and WHO drinking water standards.

Breakthrough of oxygenated water into the shallow part of the aquifer at 6SNE (5 to 12 February) is significant as the oxygen moved beyond the expected flow lines associated with the abstraction at borehole G30966. This is postulated to be due to minute gas bubbles migrating upwards to the upper part of the aquifer.

A conceptual geochemical model is described for the in-situ oxidation process using ozone/oxygen which lists the relevant oxidation-reduction couples that are of significance.

Once coherent system data becomes available (through continued data gathering and synthesis), final geochemical modelling can and will be carried out. This process at present is incomplete.

Numerous problems set out above delayed the project but it nevertheless reached the point where automatic telemetric measurements and manual field routines were providing essential data working towards achieving the research aims.

The results obtained from the field tests confirm the feasibility of in-situ iron removal at 10m from the production borehole, and although the final aim of arriving at design parameters for full scale application has not been reached the way ahead is clear and the aim is perfectly achievable in a follow-up project.

13 WAY FORWARD

The main obstacle at this stage of the project is the presumed clogging of the aquifer due to the excessive presence of the drilling mud. Repeating the step drawdown test on production borehole G30966 to test for clogging of the aquifer will be the first action to assess the situation. During the step drawdown test water levels will be recorded at as many of the deep boreholes as possible but also 10DSW for comparison with the previous test. The abstraction rate should be carefully observed.

The drilling mud decomposes via bacterial action and it should be possible to remove the breakdown products by pumping of the production borehole, but it may be advantageous to also pump the three injection boreholes to assist in the process.

Ozone (and oxygen) injection rates should be carefully measured and controlled in order to prevent the oversaturation of the groundwater with gas that may lead to bubble formation.

In order to ensure that all mechanised equipment provide meaningful readings the telemetric data should be compared with manual measurements of dissolved oxygen, water levels and all other parameters.

The mechanisation of the monitoring system and ironing out of the teething problems provided a solid and ideal basis for a continued research and arriving at the aim via geochemical modelling.

REFERENCES

Alpers, C.N. and Nordström, D.K. 1999. Geochemical modelling of water-rock interactions in mining environments. *In*: Plumlee, G.S. and Logsdon, M.J. (eds.). The environmental geochemistry of mineral deposits. Reviews in Economic Geology, 6A. Society of Economic Geologists, Chelsea, USA., pp. 89–323.

Appelo, C.A.J. and D. Postma. 1993. Geochemistry, Groundwater; and Pollution. Rotterdam, Balkema.

Appelo, C.A.J., Drijver, B., Hekkenberg, R. and de Jonge, M. (1999). Modeling *in situ* iron removal from ground water. Groundwater, 37(6), pp.811–817. Available at: http://onlinelibrary.wiley.com/doi/10.1111/j.1745-6584.1999.tb01179.x/abstract. [Accessed on 05/02/2020]

Aziz, J.S. and Hussein, O.A. (2009). Design and Implementation of a telemetry system for environmental applications. Al-Khwarizmi Engineering Journal, 5(4), pp.39–50.

Bear, J., (1979). Hydraulics of groundwater, McGraw-Hill, New York, 569 pp.

Bethke, C.M. 2008. Geochemical and biogeochemical reaction modelling, 2nd Ed. Cambridge University Press, Cambridge.

Betram, W.E., Havenga, P.L., Timmerman, K.M.G. and Vandoolaeghe, M.A.C. (1984). Atlantis: Witzand Wellfield Extension 1983. Technical Report No. Gh 3317, Division Geohydrology, DWA, Cape Town.

Braester, C. and Martinell, R. (1988). The vyredox and nitredox methods of *in-situ* treatment of groundwater. Water Science and Technology.

Bugan, R.D.H., Jovanovic, N.Z., Tredoux, G., Clarke, S., and Petersen, C. (2012). Atlantis Water Supply Scheme Support: Hydrogeological Resource Assessment. CSIR report no. SCMB 45/01/11/1.2 CSIR, Stellenbosch.

Cavé, L.C. (1997). *Inventory of Atlantis Production Boreholes*. CSIR Report No. ENV/SC97134 B, CSIR, Stellenbosch.

Cole, D.I. and Viljoen, J.H.A. (2001). Building sand potential of the Greater Cape Town area. Bulletin, Council for Geoscience, 129, 31 pp.

Crawford, J. 1999. Geochemical modelling — a review of current capabilities and future directions. SNV Report 262. Swedish Environmental Protection Agency, Stockholm, Sweden.

Department of Water (DWA) (2010). Strategy and guideline development for national groundwater planning requirements. The Atlantis Water Resource Management Scheme: 30 years of artificial groundwater recharge.

Flower, P.R. and Bishop, R.C. (2003). Atlantis Water Scheme: a case study on borehole clogging and biofouling management initiatives. Bulk Water, Water Department – The City of Cape Town.

Fleisher, J.N.E. (1990). Atlantis Groundwater Management Programme: The geohydrology of the Witzand field. CSIR Report, CSIR, Pretoria.

Hallberg, R.O. and Martinell, R. (1976). Vyredox — *In situ* purification of ground water. Ground Water, 14(2). Available at: http://dx.doi.org/10.1111/j.1745- 6584.1976.tb03638.x. [Accessed 21/11/2019]

Heath, R.C. (1983). Basic ground-water hydrology, U.S. Geological Survey Water Supply, Paper 2220, 86 pp.

Israel, S (2020). Email to Dr. Sumaya Israel, 17 January.

Klingel, F. (2016). Potential of in-situ groundwater treatment for iron, manganese and arsenic removal in. *In:* S.C. Ltd., eds. Article submitted to the 4th International Symposium Vietnam Water Cooperation Initiative for Water Security in a Changing Era, 19–20 October 2015, Hanoi, Vietnam. Hanoi, p. 10.

Kruseman, G.P. and Ridder, N.A. (2000). Analysis and evaluation of pumping test data, 2nd ed. International Institute for Land Reclamation and Improvement, Publication 47, Wagenigen.

Lohman, S.W., (1972). Ground-water hydraulics, Paper, U.S. Geological Survey, 708, 70 p.

Meyer, P.S. (2001). An explanation of the 1:500 000 general hydrogeological map Cape Town 3317. Department of Water Affairs and Forestry, Pretoria.

Minnesota Rural Water Association (MRWA) (2019). Minnesota Water Works Manual, Chapter 14: Iron and Manganese, U.S.A (accessed through website: https://www.mrwa.com/WaterWorksMnl/Chapter%2014%20Iron%20and%20Manganese.pdf). Accessed 11/02/2020]

More Water cc. (2001). *Atlantis Wellfield Rehabilitation – Consolidation Report of Phases 1 to 4*. June 2001. More Water cc., Cape Town.

Muller, J.L. and Botha, J.F. (1987). A preliminary investigation of modelling the Atlantis Aquifer. WRC Report No.113/1/87, WRC, Pretoria.

Portjanskaja, E. (2010). Ozone reactions with inorganic and organic compounds in water. Ozone Science and Technology.

Plummer, C. R., Luckett, M.D., Porter, S. and Moncrief, R (2005). Ozone sparge technology for groundwater remediation, Eco Safe Systems, USA. (http://www.ecosafeusa.com/documents/Ozone%20Documentation/Soil%20Remedi

ation/OZONE%20SPARGE%20TECHNOLOGY%20FOR%20GROUNDWATER%20REMEDIATION.pdf) [Accessed on 28/01/2020]

Reckow, A.D., Knocke, R.W., Kearney, M.J. and Parks, C.A (1991). Oxidation of iron and manganese by ozone. ozone: science and engineering. Journal of the International Ozone Association, USA.

Roberts, D.L (2001). Explanation of Sheet 3318CB (1:50 000). The geology of Melkbosstrand and Environs. Report, Council for Geoscience, Pretoria.

Roberts, D.L., Bateman, M.D., Murray-Wallace, C.V., Carr, A.S. and Holmes, P.J. (2008). West coast dune plumes: climate driven contrasts in dunefield morphogenesis along the western and southern South African coasts. Elsevier.

Robey, K. (2014). A feasibility study of in-situ iron removal in the Atlantis primary aquifer. MSc thesis, Institute of Groundwater Studies, University of the Free State, Bloemfontein.

Robey, K., Tredoux, G. and Chevallier, L. (2014). Preventing production borehole clogging by *in-situ* iron removal in South African aquifer systems. WRC Report No. 2070/1/14, WRC, Pretoria.

South African National Standards (SANS) (2015). South African National Standards for water for domestic supplies (SANS: 241-1:2015). The Council for the South African Bureau of Standards, Pretoria

Tredoux, G., and Cavè, L.C. (2002). Atlantis Aquifer. A status report on 20 years of groundwater management at Atlantis. Report, CSIR, ENV-S-C 2002-069, CSIR, Stellenbosch.

Tredoux, G., Israel, S. and Cavè, L.C. (2004). The feasibility of *in-situ* groundwater remediation as a robust low-cost water treatment option. Report, WRC, 1325/1/04, WRC, Pretoria.

Van Der Merwe, A.J. (1980). Explorasie, Ontginning en Evaluering van grondwater van die sndafsetting in die Atlantisgebied vir watervoorsiening aan die Atlantis-ontwikkelingsgebied. Technical Report No. Gh3187, Forestry and Environmental Conservation, Department of Water, Cape Town.

Van Halem, D., Heijman, S.G., Johnston, R., Huq, I.M., Ghosh S.K., Verberk J.Q., Amy G.L. and Van Dijk J.C. (2010). Subsurface iron and arsenic removal: low- cost technology for community-based water supply in Bangladesh. Water Science and Technology, 62(11), pp. 2702–2709.

Van Tonder, G.J., Botha, J.F., Chiang, W.H., Kunstmann, H. and Xu, Y. (2001). Estimation of the sustainable yields of boreholes in fractured-rock formation. Journal of Hydrogeology (Special Issue).

World Health Organisation (WHO) (2017). Guidelines for drinking-water quality: first addendum to the fourth edition.

Websites accessed: http://www.oxidationtech.com[Accessed on 17/01/2020]

APPENDIX A – WATER QUALITY DATA

Date	BH ID	Sampling and analysis result (mg/ℓ)									
		Total Fe	Total Fe*	Dissolved Fe	Total Mn	Dissolved Mn	TOC	pH	EC (µS/cm)	DO	Temp (°c)
7-Aug-19	10DNE	-	-	-	-	-	-	7.54	739	-	17.7
	G30966	-	-	-	-	-	-	8.05	686	-	18.3
1-Oct-19	10DNE	0.01	0.1	0	-	1.4	-	7.23	673	0.02	18.7
	8DNE	0.78	1.41	-	-	0.9	-	7.27	651	0.03	18.6
	6SNE	0.01	0.16	-	-	0.8	-	7.40	693	0.03	19.2
	4DNE	0.54	1.08	-	-	1.5	-	7.30	640	0.03	18.7
29-Oct-19	10DNE	0.13	-	0	-	-	15.4	7.25	704	10.90	19.4
	8DNE	0.02	0.16	0	-	0.8	-	7.10	705	8.33	19.3
	6SNE	0.01	0.03	0.05	-	0.9	-	7.60	772	0.19	19.2
	4DNE	0.03	-	0.09	-	-	15.7	7.60	650	0.17	18.9
1-Nov-19	10DNE	0.13	0.55	0	0.12	0.1	12.5	7.25	704	10.90	19.4
	8DNE	0.02	0.06	0	-	1.6	-	7.09	705	8.33	19.4
	6SNE	0.05	0.04	0.05	-	1.5	-	7.32	679	0.81	19.2
	4DNE	0.01	0.01	bdl	0.07	1.3	3	7.32	697	12.85	19.4
	G30966	0.21	0.39	0.21	-	1.6	-	7.62	703	6.70	18.8
5-Nov-19	10DNE	0.12	-	0	0.11	0.1	6.6	7.40	682	0.29	19.5
	8DNE	0.1	0.23	0.1	-	0.9	-	7.35	677	0.17	19.6
	6SNE	0.08	0.05	0.04	-	0.8	-	7.46	698	0.49	19.5
	4DNE	0.02	-	0.1	0.09	0.09	3.4	7.35	637	2.50	19.7
	G30966	0.21	0.29	0.17	-	0.8	-	7.53	689	5.20	19.6
28-Nov-19	10DNE	0.57	-	0.67	-	0.6	-	7.37	644	0.13	19.2
	8DNE	0.98	-	0.44	-	0.4	-	7.62	586	0.11	19.1
	6SNE	0.16	-	0.02	-	0.9	-	7.47	744	0.31	20.2
	4DNE	0.4	-	0.15	-	0.5	-	7.42	638	0.19	19.5
	G30966	0.52		0.14	-	0.4	-	7.52	716	2.35	19.9
2-Dec-19	10DNE	0.02	-	0	-	0.8	-	7.26	712	14.13	19.6
	8DNE	0.24	-	0.46	-	1.0	-	7.20	703	3.46	19.6
	6SNE	0.02	-	0.02	-	0.9	-	7.42	758	0.98	19.5
	4DNE	0.14	-	0.39	-	0.4	-	7.26	691	0.24	19.5
	G30966	0.24	-	0.32	-	0.4	-	7.52	721	1.83	18.9
17-Dec-19	10DNE	0.08	-	0	-	0.3	-	7.35	712	17.89	19.8
	8DNE	0.02	-	0.02	-	0.7	-	7.27	713	19.96	21.2
	6SNE	0.15	-	0	-	0.9	-	7.46	761	0.27	20.3
	4DNE	0.18	-	0.25	-	0.6	-	7.25	670	3.05	19.6
	G30966	0.21	-	0.31	-	0	-	7.54	720	5.66	19.2
21-Jan-20	10DNE	0.05	-	0	-	0.7	-	7.41	716	20.00	20.1
	8DNE	0.02	-	0	-	0.6	-	7.36	719	20.00	20.5
	6SNE	0.08	-	0	-	0.7	-	7.50	657	0.19	19.7
	4DNE	0.13	-	0.2	-	0	-	7.37	667	6.86	19.7
	G30966	0.2	-	0.32	-	1.3	-	7.63	724	5.52	19.1
29-Jan-20	10DNE	0.08	-	0	-	0.4	-	7.46	715	20.00	20.5
	8DNE	0	-	0	-	0.8	-	7.46	715	20.00	20.5
	6SNE	0.03	-	0.01	-	0.6	-	7.62	672	0.20	20.0
	4DNE	0.19	-	0.26	-	0.6	-	7.44	671	5.17	19.8
	G30966	0.21	-	0.39	-	0.5	-	7.54	722	3.49	19.0
5-Feb-20	10DNE	0.03	-	0	-	0.7	-	7.61	717	15.07	19.7
	8DNE	0.03	-	0	-	0.3	-	7.58	717	15.09	19.8
	6SNE	0	-	0	-	0.5	-	7.82	722	7.81	20.2
	4DNE	0.19	-	0.39	-	0	-	7.41	674	2.90	19.5
	G30966	0.19	-	0.41	-	0.3	-	7.58	723	2.74	19.1
12-Feb-20	10DNE	0.11	-	0.21	-	0.6	-	7.54	684	0.30	19.7
	8DNE	0.26	-	0.58	-	0.7	-	7.55	666	0.17	19.4
	6SNE	0.07	-	0	-	1.3	-	7.45	724	7.83	20.4
	4DNE	0.26	-	0.59	-	0.5	-	7.37	677	0.15	19.6
	G30966	0.19	-	0.4	-	0.3	-	7.47	723	2.63	19.8
19-Feb-20	10DNE	0.13	-	0.11	-	1.6	-	7.47	692	0.25	19.8
	8DNE	0.26	-	0.53	-	1.4	-	7.76	669	0.20	19.2
	6SNE	0.03	-	0.03	-	1.1	-	7.37	697	5.00	20.1
	4DNE	0.28	-	0.64	-	1.2	-	7.30	673	0.18	19.2
	G30966	0.21	-	0.45	-	1.4	-	7.48	719	2.38	19.2
26-Feb-20	10DNE	0.03	-	0	-	0.7	-	7.58	712	4.13	19.9
	8DNE	0.02	-	0	-	0.7	-	7.42	713	3.95	20.0
	6SNE	0.03	-	0	-	0.9	-	7.34	690	2.68	20.2
	4DNE	0.2	-	0.43	-	1.7	-	7.34	657	0.62	19.5
	G30966	0.18	-	0.45	-	0.9	-	7.49	718	2.52	19.1
4-Mar-20	10DNE	0.11	-	0.13	-	0.8	-	7.42	686	0.45	19.6
	8DNE	0.21	-	0.42	-	1.3	-	7.47	676	0.25	19.3
	6SNE	0.02	-	0.03	-	0.8	-	7.30	679	2.01	20.1
	4DNE	0.28	-	0.65	-	1.3	-	7.20	687	0.14	19.1
	G30966	0.19	-	0.46	-	0.4	-	7.55	715	5.02	19.3